RL4CO: A UNIFIED REINFORCEMENT LEARNING FOR COMBINATORIAL OPTIMIZATION LIBRARY

Anonymous authors
Paper under double-blind review

ABSTRACT

Deep reinforcement learning offers notable benefits in addressing combinatorial problems over traditional solvers, reducing the reliance on domain-specific knowledge and expert solutions, and improving computational efficiency. Despite the recent surge in interest in neural combinatorial optimization, practitioners often do not have access to a standardized code base. Moreover, different algorithms are frequently based on fragmentized implementations that hinder reproducibility and fair comparison. To address these challenges, we introduce RL4CO, a unified Reinforcement Learning (RL) for Combinatorial Optimization (CO) library. We employ state-of-the-art software and best practices in implementation, such as modularity and configuration management, to be flexible, easily modifiable, and extensible by researchers. Thanks to our unified codebase, we benchmark baseline RL solvers with different evaluation schemes on zero-shot performance, generalization, and adaptability on diverse tasks. Notably, we find that some recent methods may fall behind their predecessors depending on the evaluation settings. We hope RL4CO will encourage the exploration of novel solutions to complex real-world tasks, allowing the community to compare with existing methods through a unified framework that decouples the science from software engineering. We open-source our library at https://anonymous.4open.science/r/rl4co-iclr.

1 INTRODUCTION

Combinatorial optimization (CO) is a mathematical optimization area that encompasses a wide variety of important practical problems, such as routing problems, scheduling, and hardware design, whose solution space typically grows exponentially to the size of the problem (also often referred to as NP-hardness). As a result, CO problems can take considerable expertise to craft solvers and raw computational power to solve. Neural Combinatorial Optimization (NCO) (Bengio et al., 2021; Mazyavkina et al., 2021; Peng et al., 2021) provides breakthroughs in CO by leveraging recent advances in deep learning, especially by automating the design of solvers and considerably improving the efficiency in providing solutions. While conventional operations research (OR) approaches (Helsgaun, 2017; Vidal, 2022; David Applegate & Cook, 2023) have achieved significant progress in CO, they encounter limitations when addressing new CO tasks, as they necessitate extensive expertise. In contrast, NCO trained with reinforcement learning (RL) overcomes the limitations of OR-based approaches (i.e., manual designs) by harnessing RL's ability to learn in the absence of optimal solutions (Bello et al., 2017).[1]

NCO presents possibilities as a general problem-solving approach in CO, handling challenging problems with minimal or (almost) no dependence on problem-specific knowledge (Bello et al., 2017; Kool et al., 2019; Kwon et al., 2020; Hottung & Tierney, 2019; Barrett et al., 2020; Ahn et al., 2020a; Barrett et al., 2022). Among CO tasks, routing problems such as the Traveling Salesman Problem (TSP) and Capacitated Vehicle Routing Problem (CVRP) serve as central test suites for the capabilities of NCO due to the extensive NCO research on those types of problems (Nazari et al., 2018; Kool et al., 2019; Kwon et al., 2020; Kim et al., 2022b) and their applicability of at-hand comparison of highly dedicated heuristic solvers investigated over several decades of study by the OR

[1] Supervised learning (SL) approaches also offer notable improvements (Vinyals et al., 2015b; Lu et al., 2019; Hottung et al., 2020; Fu et al., 2020; Kool et al., 2021; Xin et al., 2021; Li et al., 2021b; Drakulic et al., 2023; Sun & Yang, 2023). However, their use is restricted due to the requirements of (near) optimal solutions during training.

community (Helsgaun, 2017; David Applegate & Cook, 2023). Recent advances (Fu et al., 2021; Li et al., 2021b; Jin et al., 2023) of NCO achieve comparable or superior performance to state-of-the-art (SOTA) solvers on these benchmarks, implying the potential of NCO to revolutionize the laborious manual design of CO solvers (Vidal, 2022; Ropke & Pisinger, 2006).

Recently, while NCO has significantly influenced the CO domain, there remains an absence of unified and flexible implementations of NCO solvers. For instance, two cornerstone NCO models, AM (Kool et al., 2019) and POMO (Kwon et al., 2020), rely on significantly different codebases that can hinder reproducibility and peer validation in the NCO domain. We believe a unified platform is crucial to advance the NCO field for both researchers and practitioners, by decoupling science from engineering and ensuring the transition from research ideas to practical applications. Furthermore, a consistent evaluation benchmark is needed; despite the usual assessment of NCO solvers based on in-training distributions, the necessity for out-of-training-distribution evaluations, reflecting real-world scenarios, is often overshadowed. Finally, there is also a need for evaluations that account for the volume of training data, as its importance has been substantiated in other ML sectors.

Contributions. In this work, we introduce RL4CO, a new reinforcement learning (RL) for combinatorial optimization (CO) benchmark. RL4CO is first and foremost a library of baselines, environments, and boilerplate from the literature implemented in a *modular*, *flexible*, and *unified* way with what we found are the best software practices and libraries, including TorchRL (Moens, 2023b), PyTorch Lightning (Falcon & The PyTorch Lightning team, 2019), Hydra (Yadan, 2019) and TensorDict (Moens, 2023a). Through our thoroughly tested unified and documented codebase, we conduct experiments to explore best practices in RL for CO and benchmark our baselines. We demonstrate that existing SOTA methods may perform poorly on different evaluation metrics and sometimes even underperform their predecessors. We also analyzed the inference schemes of NCO solvers and found that simple inference data augmentation can outperform more computationally demanding schemes, such as sampling, thanks to our unified implementation. We showcase the flexibility of RL4CO by also benchmarking lesser-studied problems in the NCO community that can be used to model real-world problems, such as non-euclidean hardware device placement (Kim et al., 2023) and constrained pickup and delivery problem (Li et al., 2021a).

2 PRELIMINARIES

The solution space of CO problems generally grows exponentially to their size. Such solution space of CO hinders the learning of NCO solvers that generate the solution in a single shot[2]. As a way to mitigate such difficulties, *autoregressive* (AR) methods as Nazari et al. (2018); Vinyals et al. (2015a); Kool et al. (2019); Kwon et al. (2020); Kim et al. (2022b) generate solutions one step at a time in an autoregressive fashion akin to language models (Brown et al., 2020; Touvron et al., 2023; OpenAI, 2023) to handle solution feasibility and constraints; in RL4CO we focus primarily on benchmarking AR approaches for given their broad applicability.

Solving Combinatorial Optimization with Autoregressive Sequence Generation AR methods construct a feasible solution as follows. They first *encodes* the problem $\boldsymbol{x}$ (e.g., For TSP, node coordinates) with trainable encoder f_θ and then *decodes* the solution $\boldsymbol{a}$ by deciding the next "action" (e.g., the next city to visit) based on the current (partial) solution using decoder g_θ, and repeating this until the solver generates the complete solution. Formally speaking,

$$\boldsymbol{h} = f_\theta(\boldsymbol{x}) \tag{1}$$

$$a_t \sim g_\theta(a_t | a_{t-1}, ..., a_0, \boldsymbol{h}) \tag{2}$$

$$p_\theta(\boldsymbol{a}|\boldsymbol{x}) \triangleq \prod_{t=1}^{T-1} g_\theta(a_t | a_{t-1}, ..., a_0, \boldsymbol{h}), \tag{3}$$

where $\boldsymbol{a} = (a_1, ..., a_T)$, T are the solution construction steps, is a feasible (and potentially optimal) solution to CO problems, $\boldsymbol{x}$ is the problem description of CO, p_θ is a (stochastic) solver that maps

[2]Also known as non-autoregressive approaches (NAR) (Joshi et al., 2021; Kool et al., 2021; Qiu et al., 2022; Gagrani et al., 2022; Xiao et al., 2023). However, imposing the feasibility of NAR-generated solutions may not be straightforward, especially for CO problems with complex constraints.

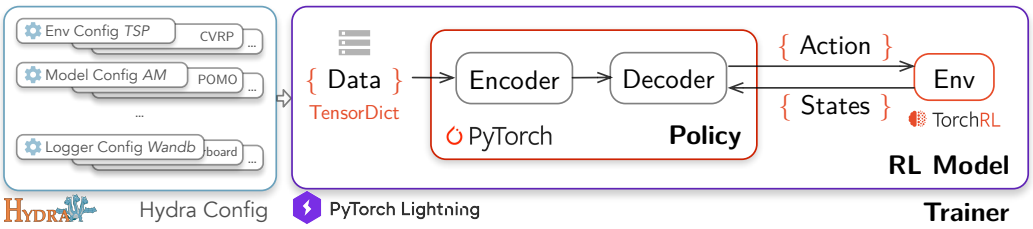

Figure 3.1: An overview of the RL4CO pipeline from configurations to training.

$\boldsymbol{x}$ to a solution $\boldsymbol{a}$. For example, for a 2D TSP with N cities, $\boldsymbol{x} = \{(x_i, y_i)\}_{i=1}^{N}$, where (x_i, y_i) is the coordinates of ith city v_i, a solution $a = (v_1, v_2, ...v_N)$.

Training NCO Solvers via Reinforcement Learning The solver p_θ can be trained with SL or RL schemes. In this work, we focus on RL solvers as they can be trained without relying on the optimal (or high-quality) solutions. Under the RL formalism, the training problem of NCOs becomes as follows:

$$\theta^* = \underset{\theta}{\operatorname{argmax}} \Big[\mathbb{E}_{\boldsymbol{x} \sim P(\boldsymbol{x})} \big[\mathbb{E}_{a \sim p_\theta(\boldsymbol{a}|\boldsymbol{x})} R(\boldsymbol{a}, \boldsymbol{x}) \big] \Big], \tag{4}$$

where $P(\boldsymbol{x})$ is problem distribution, $R(\boldsymbol{a}, \boldsymbol{x})$ is reward (i.e., the negative cost) of $\boldsymbol{a}$ given $\boldsymbol{x}$.

Eq. (4) can be solved with various RL methods including value-based (Khalil et al., 2017), policy gradient (PG) (Kool et al., 2019; Kwon et al., 2020; Kim et al., 2022b; Park et al., 2023), and actor-critic (AC) methods (Zhang et al., 2020; Park et al., 2021). In practice, we observe that explicitly training the policy (i.e., PG and AC methods) generally outperforms the value-based methods in NCO, as shown in Kool et al. (2019) and our experimental results (See § 4).

3 RL4CO

RL4CO is a unified reinforcement learning (RL) for Combinatorial Optimization (CO) library that aims to provide a *modular*, *flexible*, and *unified* code base for training and evaluating AR methods and performs extensive benchmarking capabilities on various settings. As shown in Fig. 3.1, RL4CO decouples the major components of the AR-NCO solvers and their training routine while prioritizing reusability into the following components: 1) Policy, 2) Environment, 3) RL algorithm, 4) Trainer, and 5) Configuration management.

Policy This module is for autoregressively constructing solutions. Our investigation into various AR NCO solvers has revealed common structural patterns across various CO problems. The policy network π_θ (i.e., solver) follows an architecture that combines an encoder f_θ and a decoder g_θ as follows:

$$\pi_\theta(\boldsymbol{a}|\boldsymbol{x}) \triangleq \prod_{t=1}^{T-1} g_\theta(a_t | a_{t-1}, ..., a_0, f_\theta(\boldsymbol{x})) \tag{5}$$

Upon analyzing encoder-decoder architectures, we have identified components that hinder the encapsulation of the policy from the environment. To achieve greater modularity, RL4CO modularizes such components in the form of *embeddings*: `InitEmbedding`, `ContextEmbedding` and `DynamicEmbedding`.

The encoder's primary task is to encode input $\boldsymbol{x}$ into a hidden embedding $\boldsymbol{h}$. The structure of f_θ comprises two trainable modules: the `InitEmbedding` and encoder blocks. The `InitEmbedding` module typically transforms problem features into the latent space and problem-specific compared to the encoder blocks, which often involve plain multi-head attention (MHA):

$$\boldsymbol{h} = f_\theta(\boldsymbol{x}) \triangleq \text{EncoderBlocks}(\texttt{InitEmbedding}(\boldsymbol{x})) \tag{6}$$

The decoder g_θ autoregressively constructs the solution based on the encoder output $\boldsymbol{h}$. Solution decoding involves iterative steps until a complete solution is constructed:

$$q_t = \texttt{ContextEmbedding}(\boldsymbol{h}, a_{t-1:0}), \tag{7}$$

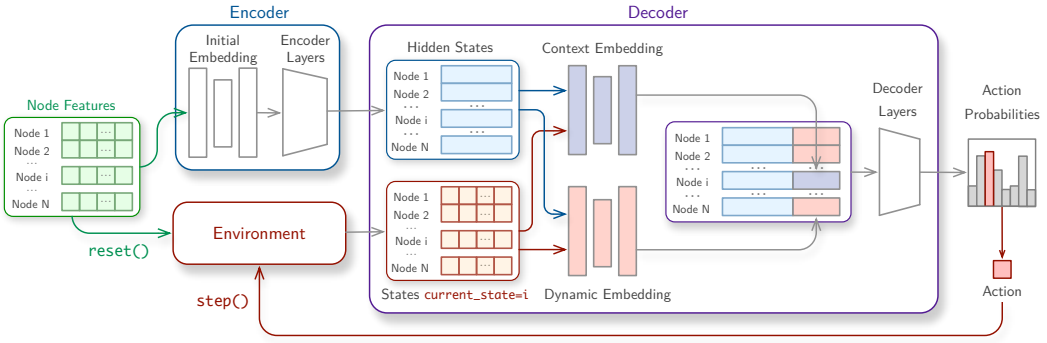

Figure 3.2: An overview of the modularized autoregressive policy in RL4CO.

$$\bar{q}_t = \text{MHA}(q_t, W_k^g \boldsymbol{h}, W_v^g \boldsymbol{h}), \tag{8}$$

$$\pi(a_t) = \text{MaskedSoftmax}(\bar{q}_t \cdot W_v \boldsymbol{h}, M_t), \tag{9}$$

where the `ContextEmbedding` is tailored to the specific problem environment, q_t and $\bar{q}_t$ represent the query and attended query (also referred to as glimpse in Mnih et al. (2014)) at the t-th decoding step, W_k^g, W_v^g and W_v are trainable linear projections computing keys and values from $\boldsymbol{h}$, and M_t denotes the action mask, which is provided by the environment to ensure solution feasibility. It is noteworthy that we also modularize the `DynamicEmbedding`, which dynamically updates the keys and values of MHA and Softmax during decoding. This approach is often used in dynamic routing settings, such as split delivery VRP. For the details, please refer to Appendix A.4.

From Eqs. (6) and (7), it is evident that creating embeddings demands problem-specific handling and often triggers coherence between the policy and CO problems. In RL4CO, we offer *plug-and-play* environment embeddings investigated from NCO literature (Kool et al., 2019; Li et al., 2021a; Kwon et al., 2021; Kim et al., 2023; Son et al., 2023) and, more importantly, allow a drop-in replacement of pre-coded embedding modules to user-defined embedding modules to attain higher modularity. Furthermore, we accommodate various decoding schemes (discussed in § 4) into a unified implementation so that those schemes can be applied to the different models, such as applying greedy multi-starts from POMO (Kwon et al., 2020) to the Attention Model (Kool et al., 2019).

Environment This module fully specifies the problem, updates the problem construction steps based on the input action, and provides the result of updates (e.g., action masks) to the policy module. When implementing the `environment`, we focus on parallel execution of rollouts (i.e., problem-solving) while maintaining *statelessness* in updating every step of solution decoding. These features are essential for ensuring the reproducibility of NCO and supporting "look-back" decoding schemes such as Monte-Carlo Tree Search. Our environment designs and implementations are flexible to accommodate various types of NCO solvers that generate a single action a_t at each decision-making step (Khalil et al., 2017; Zhang et al., 2020; Ahn et al., 2020b; Park et al., 2021; 2023). We provide further details of the benchmarked environments in Appendix C.

Our environment implementation is based on `TorchRL` (Bou et al., 2023), an open-source RL library for `PyTorch` (Paszke et al., 2017), which aims at high modularity and good runtime performance, especially on GPUs. This design choice makes the `Environment` implementation standalone, even outside of RL4CO, and consistently empowered by a community-supporting library – `TorchRL`. Moreover, we employ `TensorDicts` (Moens, 2023a) to move around data, allowing for further flexibility.

RL Algorithm This module defines the routine that takes `Environment` and its problem instances and the `Policy` and computes the gradients of θ defined by each RL algorithm such as REINFORCE, A2C, and PPO. We decouple the routines for gradient computations and parameter updates to support modern training practices in `Trainer`. We found this decoupling especially helpful in attaining higher reusability of the RL algorithms (e.g., AM, POMO, and Sym-NCO are trained with the REINFORCE algorithm but with different baselines).

Trainer Training a single NCO model is typically computationally demanding, especially since most CO problems are NP-hard. Therefore, implementing a modernized training routine becomes crucial. To this end, we implement the `Trainer` using `Lightning` (Falcon & The PyTorch Lightning team, 2019), which seamlessly supports features of modern training pipelines, including logging, checkpoint management, automatic mixed-precision training, various hardware acceleration supports (e.g., CPU, GPU, TPU, and Apple Silicon) and multi-GPU support in distributed settings (Li et al., 2020). We have found that using mixed-precision training significantly decreases training time without sacrificing NCO solver quality and enables us to leverage recent routines such as FlashAttention (Dao et al., 2022; Dao, 2023)[3].

The following code snippet shows minimalistic code that can train a model in few lines of code:

```
from rl4co.envs import TSPEnv
from rl4co.models.zoo import AttentionModel, AutoregressivePolicy
from rl4co.utils import RL4COTrainer

# Instantiate TorchRL environment
env = TSPEnv(num_loc=50)

# Create policy and RL model
policy = AutoregressivePolicy(env)
model = AttentionModel(env, policy, baseline='rollout')

# Instantiate Trainer and fit
trainer = RL4COTrainer(max_epochs=100, accelerator="gpu")
trainer.fit(model)
```

Configuration Management Optionally, but usefully, we adopt `Hydra` (Yadan, 2019), an open-source Python framework that enables hierarchical config management, making it easier to manage complex configurations and experiments with different settings.

We thoroughly test our library via continuous integration and create documentation to make it as easily accessible as possible for both newcomers and expert practitioners[4]. Installation instructions and open-source code are available at https://anonymous.4open.science/r/rl4co-iclr.

4 Experiments

4.1 Benchmark Setup

Our focus is to benchmark the NCO solvers under controlled settings, aiming to compare all benchmarked methods as closely as possible in terms of network architectures and the number of training samples consumed.

Models We evaluate the following NCO solvers[5]:

- `AM` (Kool et al., 2019) employs the multi-head attention (MHA) encoder and single-head attention decoder trained using REINFORCE and the rollout baseline.
- `POMO` (Kwon et al., 2020) utilizes the shared baseline to train AM instead of the rollout baseline.
- `Sym-NCO` (Kim et al., 2022b) utilizes the symmetric baseline to train AM instead of the rollout baseline.

[3] We investigate mixed-precision training and FlashAttention in our pipeline in Appendix E.2.

[4] Documentation: https://anonymous.4open.science/w/rl4co-iclr/_build/html/index.html.

[5] We also re-implemented PointerNetworks (Vinyals et al., 2015a; Bello et al., 2016); however, we excluded them from the main table due to their poor performance, i.e. more than 4% optimality gap in TSP50.

Table 4.1: In-distribution benchmark results for routing problems with 50 nodes. We report the gaps to the best-known solutions of classical heuristics solvers.

Method	TSP			CVRP			OP			PCTSP			PDP		
	Cost ↓	Gap	Time	Cost ↓	Gap	Time	Prize ↑	Gap	Time	Cost ↓	Gap	Time	Cost ↓	Gap	Time
Classical Solvers															
Gurobi	5.70	0.00%	2m	–	–	–	–	–	–	–	–	–	–	–	–
Concorde	5.70	0.00%	2m	–	–	–	–	–	–	–	–	–	–	–	–
HGS	–	–	–	10.37	0.00%	10h	–	–	–	–	–	–	–	–	–
Compass	–	–	–	–	–	–	16.17	0.00%	5m	–	–	–	–	–	–
LKH3	5.70	0.00%	5m	10.38	0.10%	12h	–	–	–	–	–	–	6.86	0.00%	1h30m
OR Tools	5.80	1.83%	5m	–	–	–	–	–	–	4.48	0.00%	5h	7.36	7.29%	2h
Greedy One Shot Evaluation															
A2C	5.83	2.22%	(<1s)	11.16	7.09 %	(<1s)	14.77	8.64%	(<1s)	5.15	14.96%	(<1s)	8.92	30.03%	(<1s)
AM	5.78	1.41%	(<1s)	10.95	5.30 %	(<1s)	15.46	4.40%	(<1s)	4.59	2.46%	(<1s)	7.51	9.88%	(<1s)
POMO	5.75	0.89%	(<1s)	10.80	3.99 %	(<1s)	13.86	14.26%	(<1s)	5.00	11.61%	(<1s)	7.59	10.64%	(<1s)
Sym-NCO	5.72	0.47%	(<1s)	10.87	4.61 %	(<1s)	15.67	3.09%	(<1s)	4.52	2.12%	(<1s)	7.39	7.73%	(<1s)
AM-XL	5.73	0.54%	(<1s)	10.84	4.31 %	(<1s)	15.69	2.98%	(<1s)	4.53	2.44%	(<1s)	7.31	6.56%	(<1s)
AM-PPO	5.76	0.92%	(<1s)	10.87	4.60 %	(<1s)	15.67	3.05%	(<1s)	4.55	2.45%	(<1s)	7.43	8.31%	(<1s)
Sampling with width $M = 1280$															
A2C	5.74	0.72%	40s	10.70	3.07%	1m24s	15.14	6.37%	48s	4.96	10.71%	57s	8.48	23.62%	1m15s
AM	5.72	0.40%	40s	10.60	2.22%	1m24s	15.90	1.68%	48s	4.52	0.99%	57s	7.25	5.69%	1m15s
POMO	5.71	0.18%	1m	10.54	1.64%	2m30s	14.62	9.56%	1m10s	4.82	7.59%	1m23s	7.31	6.56%	1m50s
Sym-NCO	5.70	0.14%	1m	10.58	2.03%	2m30s	16.02	0.93%	1m10s	4.52	0.82%	1m23s	7.17	4.52%	1m50s
AM-XL	5.71	0.17%	1m	10.57	1.91%	2m30s	15.97	1.25%	1m10s	4.52	0.88%	1m23s	7.15	4.23%	1m50s
AM-PPO	5.70	0.15%	1m	10.52	1.52%	1m30s	16.04	0.78%	50s	4.48	0.18%	1m	7.17	4.52%	1m20s
Greedy Multistart (N)															
A2C	5.80	1.81%	2s	10.90	4.86%	6s	14.61	9.65%	4s	5.12	14.29%	5s	8.87	29.31%	4s
AM	5.77	1.21%	2s	10.73	3.39%	6s	15.71	2.84%	4s	4.56	1.89%	5s	7.46	8.75%	4s
POMO	5.71	0.29%	3s	10.58	2.04%	8s	13.95	13.71%	7s	4.98	11.16%	7s	7.46	8.75%	6s
Sym-NCO	5.72	0.36%	3s	10.71	3.17%	8s	15.88	1.79%	7s	4.55	1.59%	7s	7.38	7.58%	6s
AM-XL	5.72	0.42%	3s	10.68	2.88%	8s	15.85	1.95%	7s	4.56	1.79%	7s	7.25	5.69%	6s
AM-PPO	5.74	0.61%	2s	10.67	2.72%	6s	15.98	1.21%	5s	4.53	1.18%	5s	7.23	5.39%	4s
Greedy with Augmentation (1280)															
A2C	5.71	0.18%	40s	10.63	2.49%	1m24s	14.89	7.91%	48s	5.15	14.96%	1m	7.91	15.31%	1m15s
AM	5.70	0.07%	40s	10.53	1.56%	1m24s	15.88	1.79%	48s	4.59	2.46%	1m	7.14	4.08%	1m15s
POMO	5.70	0.06%	1m	10.55	1.72%	2m30s	14.23	11.97%	1m15m	5.09	13.61%	1m42s	7.15	4.23%	1m45s
Sym-NCO	5.70	0.01%	1m	10.53	1.54%	2m30s	15.94	1.41%	1m15m	4.58	2.17%	1m42s	7.03	2.48%	1m45s
AM-XL	5.70	0.01%	1m	10.52	1.47%	2m30s	15.90	1.66%	1m15m	4.59	2.54%	1m42s	6.98	1.75%	1m45s
AM-PPO	5.70	0.15%	42m	10.52	1.52%	1m30s	16.01	0.84%	52s	4.48	0.18%	1m5s	7.00	2.04%	1m20s
Greedy Multistart with Augmentation ($N \times 16$)															
A2C	5.72	0.41%	32s	10.67	2.81%	1m	15.22	5.88%	30s	5.06	12.94%	35s	7.88	14.87%	50s
AM	5.71	0.21%	32s	10.55	1.73%	1m	16.05	0.76%	30s	4.54	1.28%	35s	7.10	3.50%	50s
POMO	5.70	0.05%	48s	10.48	1.11%	2m	15.05	6.94%	1m	4.92	9.81%	1m20s	7.12	3.79%	1m25
Sym-NCO	5.70	0.03%	48s	10.54	1.63%	2m	16.09	0.51%	1m	4.53	1.17%	1m20s	7.01	2.19%	1m25
AM-XL	5.70	0.04%	48s	10.53	1.50%	2m	16.08	0.57%	1m	4.54	1.25%	1m20s	7.00	2.04%	1m25
AM-PPO	5.70	0.03%	35s	10.51	1.45%	1m	16.09	0.49%	35s	4.49	0.89%	38s	6.98	1.75%	55m

- `AM-XL` is AM that adopts `POMO`-style MHA encoder, using six MHA layers and InstanceNorm instead of BatchNorm. We train `AM-XL` on the same number of samples as `POMO`.
- `A2C` is a variant of AM trained with Advantage Actor-Critic (A2C). It evaluates the rewards using the learned critic during training. We adopt Kool et al. (2019)'s implementation.
- `AM-PPO` is an A2C model trained with Proximal Policy Optimization (PPO, Schulman et al. (2017)) algorithm.

For fairness of comparison, we try to match the number of training steps to be the same and adjust the batch size accordingly. Specifically, we train models for 100 epochs as in Kool et al. (2019) using the Adam optimizer (Kingma & Ba, 2014) with an initial learning rate (LR) of 0.001 with a decay factor of 0.1 after the 80th and 95th epochs[6]. We provide additional details in Appendix D.

Environments We benchmark the NCO solvers on canonical routing problems: the Traveling Salesman Problem (TSP), the Capacitated Vehicle Routing Problem (CVRP), the Orienteering Problem (OP), and the Prize Collecting TSP (PCTSP), as evaluated in Kool et al. (2019). Additionally, we examine a relatively underexplored problem that often arises in real world applications, the Pickup and Delivery Problem (PDP), following the implementation of Li et al. (2021a). We also benchmark the Decap Placement Problems (DPP) from electronic design automation in Appendix B. Further details on environment implementations and data generation are provided in Appendix C.

[6]We find that simple learning rate scheduling with `MultiStepLinear` can improve performance i.e., compared to the original AM implementation.

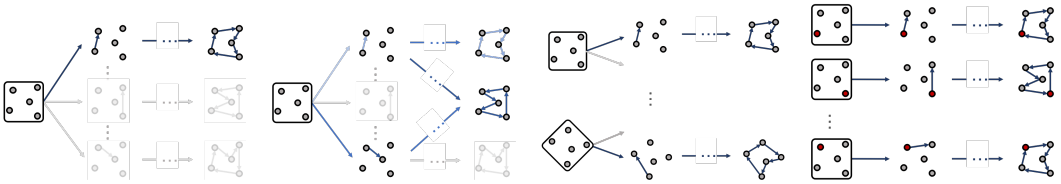

(a) Greedy (b) Sampling (c) Augmentation (d) Multistart

Figure 4.1: Decoding schemes of the autoregressive NCO solvers evaluated in this paper.

Decoding Schemes The solution quality of NCO solvers often shows large variations in performances to the different decoding schemes, even though using the same NCO solvers. Regarding that, we evaluate the trained solvers using five schemes shown in Fig. 4.1:

- `Greedy`: elects the highest probabilities at each decoding step.
- `Sampling`: concurrently samples N solutions using a trained stochastic policy.
- `Multistart Greedy`: inspired by POMO, decodes from the first given nodes and considers the best results from N cases starting at N different cities. For example, in TSP with N nodes, a single problem involves starting from N different cities.
- `Augmentation`: selects the best greedy solutions from randomly augmented problems (e.g., random rotation and flipping) during evaluation.
- `Multistart Greedy + Augmentation`: combines Multistart Greedy and Augmentation.

4.2 Benchmark Results

In-distribution We first measure the performances of NCO solvers on the same dataset distribution on which they are trained. The results for training on 50 nodes are summarized in Table 4.1. We first observe that, counter to the commonly known trends that AM < POMO < Sym-NCO, the trends can change to decoding schemes and targeting CO problems. Especially when the solver decodes the solutions with `Augmentation` or `Greedy Multistart + Augmentation`, the performance differences among the benchmarked solvers on TSP and CVRP become less significant.

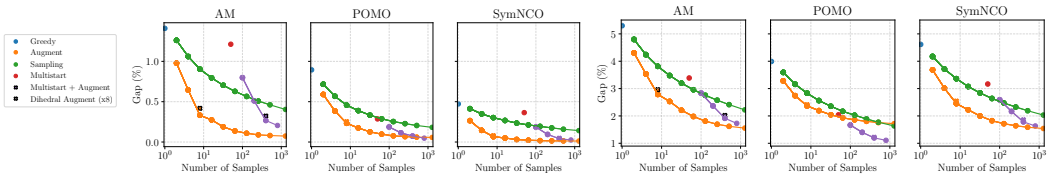

Figure 4.2: Pareto front of decoding schemes by number of samples. Left: TSP50; right: CVRP50.

We note that the original implementation of POMO [7] is not directly applicable to OP, PCTSP and PDP. Adapting it to solve new problems is not straightforward due to the coupling between environment and policy implementations. However, owing to the flexibility of RL4CO, we successfully implemented POMO for OP and PCTSP. Our results indicate that POMO underperforms in OP and PCTSP; unlike TSP, CVRP, and PDP, where all nodes need to be visited, OP and PCTSP are not constrained to visit all nodes. Due to such differences, POMO's visiting all nodes strategy may not work as an effective inductive bias. Further, we benchmark the NCO solvers for PDP, which is not originally supported natively by each of the benchmarked solvers. We apply the environment embeddings and the Heterogeneous Attention Encoder from HAM (Li et al., 2021a) to the NCO models for encoding pickup and delivery pairs, further emphasizing RL4CO's flexibility. We observe that AM-XL, which employs the same RL algorithm as AM but features the encoder architecture of POMO and is trained with an equivalent number of samples, yields performance comparable to NCO solvers using more sophisticated baselines. This suggests that careful controls on architecture and the number of training samples are required when evaluating NCO solvers.

[7] https://github.com/yd-kwon/POMO

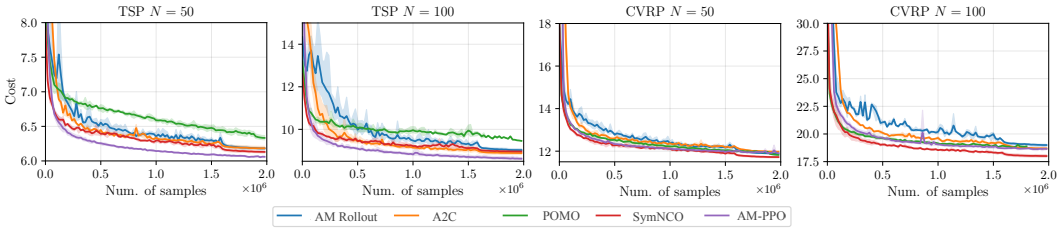

Figure 4.3: Validation cost curves and number of training samples consumed. Models with greater performance after full training may show worse convergence properties when number of training samples is limited.

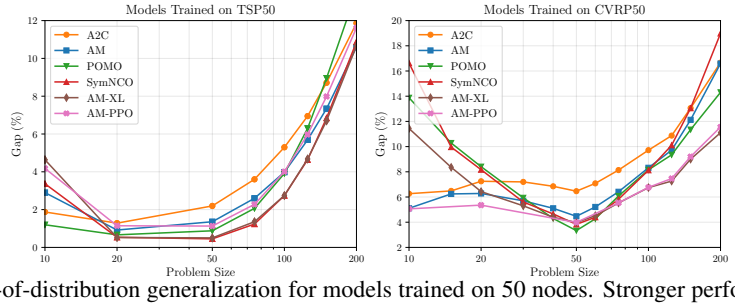

Figure 4.4: Out-of-distribution generalization for models trained on 50 nodes. Stronger performance in distribution does not always translate to out-of-distribution.

During inference, investing more computational resources (i.e., increasing the number of samples), the trained NCO solver can discover improved solutions. We examine the performance gains achieved with varying numbers of samples. As shown in Fig. 4.2, the `Augmentation` decoding scheme achieves the Pareto front with limited samples and, notably, generally outperforms other decoding schemes.

We also evaluate the NCO solvers based on the number of training samples (i.e., the number of reward evaluations). As shown in Fig. 4.3, we found that actor-critic methods (e.g., A2C and PPO) can exhibit efficacy in scenarios with limited training samples, as demonstrated by the TSP50/100 results in Fig. 4.3. This observation suggests that NCO solvers with control over the number of samples may exhibit a different trend from the commonly recognized trends. In the extension of this viewpoint, we conducted additional benchmarking in a different problem domain: electronic design automation (EDA) - detailed in Appendix B - where reward evaluation is resource-intensive due to the necessity of electrical simulations, in which sample efficiency becomes even more crucial.

Out-of-distribution In this section, we evaluate the out-of-distribution performance of the NCO solvers by measuring the optimality gap compared to the best-known tractable solver. The evaluation results are visualized in Fig. 4.4. Contrary to the in-distribution results, we find that NCO solvers with sophisticated baselines (i.e., POMO and Sym-NCO) tend to exhibit worse generalization when the problem size changes, either for solving smaller or larger instances. This can be seen as an indication of "overfitting" to the training sizes. On the other hand, variants of AM show relatively better generalization results overall. We also evaluate the solvers in two canonical public benchmark instances (TSPLib and CVRPLib) in Appendix F, which exhibit both variations in the number of nodes as well as their distributions and find a similar trend.

Search methods One viable and prominent approach of NCO that mitigates distributional shift (e.g., the size of problems) is the (learnable) search methods, which involve training (a part of) a pre-trained NCO solver to adapt to CO instances of interest. We implement and evaluate the following search methods:

- `AS`: Active Search from Bello et al. (2017) finetunes a pre-trained model on the searched instances by adapting all the policy parameters.
- `EAS`: Efficient Active Search from Hottung et al. (2022) finetunes a subset of parameters (i.e., embeddings or new layers) and adds an imitation learning loss to improve convergence.

Table 4.2: Search Methods results of models pre-trained on 50 nodes. *Classic* refers to Concorde (David Applegate & Cook, 2023) for TSP and HGS (Vidal, 2022) for CVRP. OOM denotes "Out of Memory".

Type	Metric	TSP						CVRP					
		POMO			Sym-NCO			POMO			Sym-NCO		
		200	500	1000	200	500	1000	200	500	1000	200	500	1000
Classic	Cost	10.17	16.54	23.13	10.72	16.54	23.13	27.95	63.45	120.47	27.95	63.45	120.47
Zero-shot	Cost	13.15	29.96	58.01	13.30	29.42	56.47	29.16	92.30	141.76	32.75	86.82	190.69
	Gap[%]	29.30	81.14	150.80	24.07	77.87	144.14	4.33	45.47	17.67	17.17	36.83	58.29
	Time[s]	2.52	11.87	96.30	2.70	13.19	104.91	1.94	15.03	250.71	2.93	15.86	150.69
AS	Cost	11.16	20.03	OOM	11.92	22.41	OOM	28.12	63.98	OOM	28.51	66.49	OOM
	Gap[%]	4.13	21.12	OOM	11.21	35.48	OOM	0.60	0.83	OOM	2.00	4.79	OOM
	Time[s]	7504	10070	OOM	7917	10020	OOM	8860	21305	OOM	9679	24087	OOM
EAS	Cost	11.10	20.94	35.36	11.65	22.80	38.77	28.10	64.74	125.54	29.25	70.15	140.97
	Gap[%]	3.55	26.64	52.89	8.68	37.86	67.63	0.52	2.04	4.21	4.66	10.57	17.02
	Time[s]	348	1562	13661	376	1589	14532	432	1972	20650	460	2051	17640

We apply AS and EAS to POMO and Sym-NCO pre-trained on TSP and CVRP with 50 nodes to solve larger instances having $N \in [200, 500, 1000]$ nodes. As shown in Table 4.2, solvers with search methods improve the solution quality. However, POMO generally shows better improvements over Sym-NCO. This suggests once more that the "overfitting" of sophisticated baselines can perform better in-training distributions but eventually worse in different downstream tasks.

4.3 Discussion

Limitations In this paragraph we identify some limitations and areas of improvement with our current library and benchmark experiments. Regarding benchmarking experiments, we mainly focus on training the solvers on relatively smaller sizes due to our limited computational budget. We also focus mainly on benchmarking the change of sizes rather than the change of data-generating distribution as in Bi et al. (2022), which could yield interesting results - although we do benchmark real-world instances of TSPLib and CVRPLib that include both new size and data distributions. In terms of the RL4CO library, we prioritized implementing RL AR approaches due to their flexibility, even though NAR approaches such as the ones trained with SL show good generalization performance in relatively less constrained routing problems as TSP (Joshi et al., 2019; Sun & Yang, 2023), although they require labeled solution datasets.

Future Directions in RL4CO As extensions of RL4CO library, we plan to support more methods aside from AR approaches. Given that recent NAR models often decode solutions in an AR manner to enforce the feasibility of the generated solutions, we are expecting supporting NAR methods (Kool et al., 2021; Xiao et al., 2023) would be possible under a unified manner in RL4CO. Improvement heuristics (Wu et al., 2021), which learn to improve suboptimal complete solutions (Hou et al., 2023; Xin et al., 2021; Kim et al., 2021; 2022a; Ye et al., 2023) are also an interesting future direction we would like to pursue. Such improvement heuristics would serve as useful toolkits for researchers and practitioners as they are applicable on top of existing NCO solvers with anytime-ness (i.e., can limit the runtime while having complete solutions). Furthermore, hybrid approaches that divide and conquer problems (Kim et al., 2021; Hou et al., 2023) via global and local policies are an exciting avenue for future works. Finally, we would like to support a wider variety of real-world problems, such as routing problems with soft/hard time windows.

5 Conclusion

This paper introduces RL4CO, a modular, flexible, and unified Reinforcement Learning (RL) for Combinatorial Optimization (CO) library. Our software library aims to fill the gap in unifying implementations for NCO by utilizing several best practices with the goal of providing researchers and practitioners with a flexible starting point for NCO research. With RL4CO, we benchmarked NCO solvers with experiments showing that a comparison of NCO solvers across different metrics and tasks is fundamental, as state-of-the-art approaches may perform worse than predecessors depending on specific settings. We hope that our benchmark library will provide a solid starting point for NCO researchers to explore new avenues and drive advancements.

REFERENCES

Sungsoo Ahn, Junsu Kim, Hankook Lee, and Jinwoo Shin. Guiding deep molecular optimization with genetic exploration. *Advances in neural information processing systems*, 33:12008–12021, 2020a.

Sungsoo Ahn, Younggyo Seo, and Jinwoo Shin. Learning what to defer for maximum independent sets. In *International Conference on Machine Learning*, pp. 134–144. PMLR, 2020b.

Thomas Barrett, William Clements, Jakob Foerster, and Alex Lvovsky. Exploratory combinatorial optimization with reinforcement learning. In *Proceedings of the AAAI Conference on Artificial Intelligence*, volume 34, pp. 3243–3250, 2020.

Thomas D Barrett, Christopher WF Parsonson, and Alexandre Laterre. Learning to solve combinatorial graph partitioning problems via efficient exploration. *arXiv preprint arXiv:2205.14105*, 2022.

Irwan Bello, Hieu Pham, Quoc V Le, Mohammad Norouzi, and Samy Bengio. Neural combinatorial optimization with reinforcement learning. *arXiv preprint arXiv:1611.09940*, 2016.

Irwan Bello, Hieu Pham, Quoc V. Le, Mohammad Norouzi, and Samy Bengio. Neural combinatorial optimization with reinforcement learning, 2017.

Yoshua Bengio, Andrea Lodi, and Antoine Prouvost. Machine learning for combinatorial optimization: a methodological tour d'horizon. *European Journal of Operational Research*, 290(2): 405–421, 2021.

Jieyi Bi, Yining Ma, Jiahai Wang, Zhiguang Cao, Jinbiao Chen, Yuan Sun, and Yeow Meng Chee. Learning generalizable models for vehicle routing problems via knowledge distillation. *Advances in Neural Information Processing Systems*, 35:31226–31238, 2022.

Ekaba Bisong and Ekaba Bisong. Google colaboratory. *Building machine learning and deep learning models on google cloud platform: a comprehensive guide for beginners*, pp. 59–64, 2019.

Albert Bou, Matteo Bettini, Sebastian Dittert, Vikash Kumar, Shagun Sodhani, Xiaomeng Yang, Gianni De Fabritiis, and Vincent Moens. TorchRL: A data-driven decision-making library for PyTorch. In *arXiv*, 2023. URL https://arxiv.org/abs/2306.00577.

Greg Brockman, Vicki Cheung, Ludwig Pettersson, Jonas Schneider, John Schulman, Jie Tang, and Wojciech Zaremba. Openai gym. *arXiv preprint arXiv:1606.01540*, 2016.

Tom Brown, Benjamin Mann, Nick Ryder, Melanie Subbiah, Jared D Kaplan, Prafulla Dhariwal, Arvind Neelakantan, Pranav Shyam, Girish Sastry, Amanda Askell, et al. Language models are few-shot learners. *Advances in neural information processing systems*, 33:1877–1901, 2020.

Tri Dao. Flashattention-2: Faster attention with better parallelism and work partitioning. *arXiv preprint arXiv:2307.08691*, 2023.

Tri Dao, Dan Fu, Stefano Ermon, Atri Rudra, and Christopher Ré. Flashattention: Fast and memory-efficient exact attention with io-awareness. *Advances in Neural Information Processing Systems*, 35:16344–16359, 2022.

Vašek Chvátal David Applegate, Robert Bixby and William Cook. Concorde tsp solver, 2023. URL https://www.math.uwaterloo.ca/tsp/concorde/index.html.

Darko Drakulic, Sofia Michel, Florian Mai, Arnaud Sors, and Jean-Marc Andreoli. Bq-nco: Bisimulation quotienting for generalizable neural combinatorial optimization. *Advances in Neural Information Processing Systems*, 2023.

William Falcon and The PyTorch Lightning team. PyTorch Lightning, 3 2019. URL https://github.com/Lightning-AI/lightning.

Matteo Fischetti, Juan Jose Salazar Gonzalez, and Paolo Toth. Solving the orienteering problem through branch-and-cut. *INFORMS Journal on Computing*, 10(2):133–148, 1998.

Zhang-Hua Fu, Kai-Bin Qiu, and Hongyuan Zha. Generalize a small pre-trained model to arbitrarily large tsp instances, 2020.

Zhang-Hua Fu, Kai-Bin Qiu, and Hongyuan Zha. Generalize a small pre-trained model to arbitrarily large tsp instances. In *Proceedings of the AAAI conference on artificial intelligence*, volume 35, pp. 7474–7482, 2021.

Mukul Gagrani, Corrado Rainone, Yang Yang, Harris Teague, Wonseok Jeon, Roberto Bondesan, Herke van Hoof, Christopher Lott, Weiliang Zeng, and Piero Zappi. Neural topological ordering for computation graphs. *Advances in Neural Information Processing Systems*, 35:17327–17339, 2022.

Bruce L Golden, Larry Levy, and Rakesh Vohra. The orienteering problem. *Naval Research Logistics (NRL)*, 34(3):307–318, 1987.

LLC Gurobi Optimization. Gurobi optimizer reference manual, 2021. URL http://www.gurobi.com.

Keld Helsgaun. An extension of the lin-kernighan-helsgaun tsp solver for constrained traveling salesman and vehicle routing problems. *Roskilde: Roskilde University*, 12 2017. doi: 10.13140/RG.2.2.25569.40807.

André Hottung and Kevin Tierney. Neural large neighborhood search for the capacitated vehicle routing problem. *CoRR*, abs/1911.09539, 2019. URL http://arxiv.org/abs/1911.09539.

André Hottung, Bhanu Bhandari, and Kevin Tierney. Learning a latent search space for routing problems using variational autoencoders. In *International Conference on Learning Representations*, 2020.

André Hottung, Yeong-Dae Kwon, and Kevin Tierney. Efficient active search for combinatorial optimization problems. *International conference on learning representations*, 2022.

Qingchun Hou, Jingwei Yang, Yiqiang Su, Xiaoqing Wang, and Yuming Deng. Generalize learned heuristics to solve large-scale vehicle routing problems in real-time. In *The Eleventh International Conference on Learning Representations*, 2023.

Jisoo Hwang, Jun So Pak, Dooseok Yoon, Heeseok Lee, James Jeong, Yun Heo, and Ilryong Kim. Enhancing on-die pdn for optimal use of package pdn with decoupling capacitor. In *2021 IEEE 71st Electronic Components and Technology Conference (ECTC)*, pp. 1825–1830, 2021. doi: 10.1109/ECTC32696.2021.00288.

Lima Ivan. Capacitated vehicle routing problem library. http://vrp.atd-lab.inf.puc-rio.br/index.php/en/. 2014.

Yan Jin, Yuandong Ding, Xuanhao Pan, Kun He, Li Zhao, Tao Qin, Lei Song, and Jiang Bian. Pointerformer: Deep reinforced multi-pointer transformer for the traveling salesman problem. *Proceedings of the AAAI Conference on Artificial Intelligence*, 37(7):8132–8140, Jun. 2023. doi: 10.1609/aaai.v37i7.25982. URL https://ojs.aaai.org/index.php/AAAI/article/view/25982.

Chaitanya K Joshi, Thomas Laurent, and Xavier Bresson. An efficient graph convolutional network technique for the travelling salesman problem. *arXiv preprint arXiv:1906.01227*, 2019.

Chaitanya K Joshi, Quentin Cappart, Louis-Martin Rousseau, and Thomas Laurent. Learning tsp requires rethinking generalization. In *27th International Conference on Principles and Practice of Constraint Programming (CP 2021)*. Schloss Dagstuhl-Leibniz-Zentrum für Informatik, 2021.

Jack Juang, Ling Zhang, Zurab Kiguradze, Bo Pu, Shuai Jin, and Chulsoon Hwang. A modified genetic algorithm for the selection of decoupling capacitors in pdn design. In *2021 IEEE International Joint EMC/SI/PI and EMC Europe Symposium*, pp. 712–717, 2021. doi: 10.1109/EMC/SI/PI/EMCEurope52599.2021.9559292.

Elias Khalil, Hanjun Dai, Yuyu Zhang, Bistra Dilkina, and Le Song. Learning combinatorial optimization algorithms over graphs. *Advances in neural information processing systems*, 30, 2017.

Haeyeon Kim, Minsu Kim, Federico Berto, Joungho Kim, and Jinkyoo Park. DevFormer: A symmetric transformer for context-aware device placement. *International Conference on Machine Learning*, 2023.

Minjun Kim, Junyoung Park, and Jinkyoo Park. Learning to cross exchange to solve min-max vehicle routing problems. In *The Eleventh International Conference on Learning Representations*, 2022a.

Minsu Kim, Jinkyoo Park, and Joungho Kim. Learning collaborative policies to solve np-hard routing problems. In *Advances in Neural Information Processing Systems*, 2021.

Minsu Kim, Junyoung Park, and Jinkyoo Park. Sym-NCO: Leveraging symmetricity for neural combinatorial optimization. *Advances in Neural Information Processing Systems*, 2022b.

Diederik P Kingma and Jimmy Ba. Adam: A method for stochastic optimization. *arXiv preprint arXiv:1412.6980*, 2014.

Wouter Kool, Herke Van Hoof, and Max Welling. Attention, learn to solve routing problems! *International Conference on Learning Representations*, 2019.

Wouter Kool, Herke van Hoof, Joaquim A. S. Gromicho, and Max Welling. Deep policy dynamic programming for vehicle routing problems. *CoRR*, abs/2102.11756, 2021. URL https://arxiv.org/abs/2102.11756.

Yeong-Dae Kwon, Jinho Choo, Byoungjip Kim, Iljoo Yoon, Youngjune Gwon, and Seungjai Min. POMO: Policy optimization with multiple optima for reinforcement learning. *Advances in Neural Information Processing Systems*, 33:21188–21198, 2020.

Yeong-Dae Kwon, Jinho Choo, Iljoo Yoon, Minah Park, Duwon Park, and Youngjune Gwon. Matrix encoding networks for neural combinatorial optimization. *Advances in Neural Information Processing Systems*, 34:5138–5149, 2021.

Jingwen Li, Liang Xin, Zhiguang Cao, Andrew Lim, Wen Song, and Jie Zhang. Heterogeneous attentions for solving pickup and delivery problem via deep reinforcement learning. *IEEE Transactions on Intelligent Transportation Systems*, 23(3):2306–2315, 2021a.

Shen Li, Yanli Zhao, Rohan Varma, Omkar Salpekar, Pieter Noordhuis, Teng Li, Adam Paszke, Jeff Smith, Brian Vaughan, Pritam Damania, et al. Pytorch distributed: Experiences on accelerating data parallel training. *arXiv preprint arXiv:2006.15704*, 2020.

Sirui Li, Zhongxia Yan, and Cathy Wu. Learning to delegate for large-scale vehicle routing. *Advances in Neural Information Processing Systems*, 34, 2021b.

Hao Lu, Xingwen Zhang, and Shuang Yang. A learning-based iterative method for solving vehicle routing problems. In *International conference on learning representations*, 2019.

Nina Mazyavkina, Sergey Sviridov, Sergei Ivanov, and Evgeny Burnaev. Reinforcement learning for combinatorial optimization: A survey. *Computers & Operations Research*, 134:105400, 2021.

Volodymyr Mnih, Nicolas Heess, Alex Graves, et al. Recurrent models of visual attention. *Advances in neural information processing systems*, 27, 2014.

Vincent Moens. TensorDict: your PyTorch universal data carrier, 2023a. URL https://github.com/pytorch-labs/tensordict.

Vincent Moens. TorchRL: an open-source Reinforcement Learning (RL) library for PyTorch, 2023b. URL https://github.com/pytorch/rl.

Samuel A Mulder and Donald C Wunsch II. Million city traveling salesman problem solution by divide and conquer clustering with adaptive resonance neural networks. *Neural Networks*, 16 (5-6):827–832, 2003.

Mohammadreza Nazari, Afshin Oroojlooy, Lawrence Snyder, and Martin Takác. Reinforcement learning for solving the vehicle routing problem. *Advances in neural information processing systems*, 31, 2018.

OpenAI. GPT-4 technical report, 2023.

Long Ouyang, Jeffrey Wu, Xu Jiang, Diogo Almeida, Carroll Wainwright, Pamela Mishkin, Chong Zhang, Sandhini Agarwal, Katarina Slama, Alex Ray, et al. Training language models to follow instructions with human feedback. *Advances in Neural Information Processing Systems*, 35: 27730–27744, 2022.

Matteo Pagliardini, Daniele Paliotta, Martin Jaggi, and François Fleuret. Faster causal attention over large sequences through sparse flash attention. *arXiv preprint arXiv:2306.01160*, 2023.

Junyoung Park, Jaehyeong Chun, Sang Hun Kim, Youngkook Kim, and Jinkyoo Park. Learning to schedule job-shop problems: representation and policy learning using graph neural network and reinforcement learning. *International Journal of Production Research*, 59(11):3360–3377, 2021.

Junyoung Park, Changhyun Kwon, and Jinkyoo Park. Learn to solve the min-max multiple traveling salesmen problem with reinforcement learning. In *Proceedings of the 2023 International Conference on Autonomous Agents and Multiagent Systems*, pp. 878–886, 2023.

Adam Paszke, Sam Gross, Soumith Chintala, Gregory Chanan, Edward Yang, Zachary DeVito, Zeming Lin, Alban Desmaison, Luca Antiga, and Adam Lerer. Automatic differentiation in pytorch. In *NIPS-W*, 2017.

Adam Paszke, Sam Gross, Francisco Massa, Adam Lerer, James Bradbury, Gregory Chanan, Trevor Killeen, Zeming Lin, Natalia Gimelshein, Luca Antiga, et al. Pytorch: An imperative style, high-performance deep learning library. *Advances in neural information processing systems*, 32, 2019.

Yun Peng, Byron Choi, and Jianliang Xu. Graph learning for combinatorial optimization: a survey of state-of-the-art. *Data Science and Engineering*, 6(2):119–141, 2021.

Laurent Perron and Vincent Furnon. Or-tools, 2023. URL https://developers.google.com/optimization/.

Ruizhong Qiu, Zhiqing Sun, and Yiming Yang. DIMES: A differentiable meta solver for combinatorial optimization problems. *arXiv preprint arXiv:2210.04123*, 2022.

Gerhard Reinelt. Tsplib—a traveling salesman problem library. *ORSA journal on computing*, 3(4): 376–384, 1991.

Stefan Ropke and David Pisinger. An adaptive large neighborhood search heuristic for the pickup and delivery problem with time windows. *Transportation science*, 40(4):455–472, 2006.

John Schulman, Filip Wolski, Prafulla Dhariwal, Alec Radford, and Oleg Klimov. Proximal policy optimization algorithms. *arXiv preprint arXiv:1707.06347*, 2017.

Jiwoo Son, Minsu Kim, Sanghyeok Choi, and Jinkyoo Park. Solving np-hard min-max routing problems as sequential generation with equity context. *arXiv preprint arXiv:2306.02689*, 2023.

Zhiqing Sun and Yiming Yang. Difusco: Graph-based diffusion solvers for combinatorial optimization. *arXiv preprint arXiv:2302.08224*, 2023.

Hugo Touvron, Thibaut Lavril, Gautier Izacard, Xavier Martinet, Marie-Anne Lachaux, Timothée Lacroix, Baptiste Rozière, Naman Goyal, Eric Hambro, Faisal Azhar, et al. Llama: Open and efficient foundation language models. *arXiv preprint arXiv:2302.13971*, 2023.

Thibaut Vidal. Hybrid genetic search for the cvrp: Open-source implementation and swap* neighborhood. *Computers & Operations Research*, 140:105643, 2022.

Oriol Vinyals, Meire Fortunato, and Navdeep Jaitly. Pointer networks. In C. Cortes, N. Lawrence, D. Lee, M. Sugiyama, and R. Garnett (eds.), *Advances in Neural Information Processing Systems*, volume 28, pp. 2692–2700. Curran Associates, Inc., 2015a. URL https://proceedings.neurips.cc/paper/2015/file/29921001f2f04bd3baee84a12e98098f-Paper.pdf.

Oriol Vinyals, Meire Fortunato, and Navdeep Jaitly. Pointer networks. *Advances in neural information processing systems*, 28, 2015b.

Yaoxin Wu, Wen Song, Zhiguang Cao, Jie Zhang, and Andrew Lim. Learning improvement heuristics for solving routing problems. *IEEE transactions on neural networks and learning systems*, 33(9):5057–5069, 2021.

Yubin Xiao, Di Wang, Huanhuan Chen, Boyang Li, Wei Pang, Xuan Wu, Hao Li, Dong Xu, Yanchun Liang, and You Zhou. Reinforcement learning-based non-autoregressive solver for traveling salesman problems. *arXiv preprint arXiv:2308.00560*, 2023.

Liang Xin, Wen Song, Zhiguang Cao, and Jie Zhang. Neurolkh: Combining deep learning model with lin-kernighan-helsgaun heuristic for solving the traveling salesman problem. *Advances in Neural Information Processing Systems*, 34, 2021.

Omry Yadan. Hydra - a framework for elegantly configuring complex applications. Github, 2019. URL https://github.com/facebookresearch/hydra.

Haoran Ye, Jiarui Wang, Zhiguang Cao, Helan Liang, and Yong Li. Deepaco: Neural-enhanced ant systems for combinatorial optimization. *arXiv preprint arXiv:2309.14032*, 2023.

Cong Zhang, Wen Song, Zhiguang Cao, Jie Zhang, Puay Siew Tan, and Xu Chi. Learning to dispatch for job shop scheduling via deep reinforcement learning. *Advances in Neural Information Processing Systems*, 33:1621–1632, 2020.

A Additional Discussion about the RL4CO Library

A.1 Why Choosing RL4CO?

In this paper, we introduce RL4CO, a *modular*, *flexible*, and *unified* implementation of NCO. In designing the library, we intended RL4CO to be used for various purposes ranging from research to production. RL4CO enables the users to have the following benefits.

Figure A.1: RL4CO logo.

Minimal Implementation of Boilerplate Codes for NCO As with the other RL projects, implementation of NCO with RL involves designing and coding the systems composed mainly of agents (i.e., policy) and environment (i.e., CO problem). However, this often involves a serious amount of engineering, especially to attain higher executions in training routines. Moreover, we found that a significant chunk of NCO solvers are based on AM or POMO implementation and the subroutines that have been done in the implementation. Regarding those practical aspects, RL4CO provides a modularized code base for each routine of NCO, including environment, policy network architecture, RL algorithm, and training. So that the users can easily mix and match SoTA NCO practices and user-defined modules while having full control over the entire RL pipeline.

Easier Comparison Among NCO Algorithms Current NCO research shows a tendency to rely on two cornerstone implementations: AM and POMO. However, due to differences in implementation (e.g., network architecture, training scheme), direct head-to-head comparisons among the algorithms might not be straightforward. For example, applying POMO's state augmentation to AM's policy to reveal the effect of augmentation from the baseline selections can be challenging. RL4CO provides a unified implementation of NCO models (and their subroutines) to offer higher adaptability of routines from one algorithm to another. We believe this will promote easier comparisons among the models while developing novel NCO solvers to address various CO problems.

Leveraging Standardized Open-Source Libraries During the development of RL4CO, we have decided to utilize standardized and reputable open-source libraries based on extensive research and expertise at the edge of software engineering and research, such as the recent TorchRL (Bou et al., 2023) and the `TensorDict` data structure from Moens (2023a). We believe these design choices will yield various practical benefits both in research and production. For instance, by disentangling the RL algorithm from the training subroutines of RL4CO, NCO solvers can undergo training using an array of state-of-the-art training methods supported by PyTorch Lightning (Falcon & The PyTorch Lightning team, 2019). Additionally, deploying the trained NCO solvers to production becomes seamless through the utilization of tools such as TorchServe, to name just a couple of examples.

A.2 On the Choice of the Software Backbone

During the development of RL4CO, we wanted to make it as simple as possible to integrate reproducible and standardized code adhering to the latest guidelines. As a main template for our codebase, we use Lightning-Hydra-Template [8] which we acknowledge being a solid starting point for reproducible deep learning. We further discuss framework choices below.

TorchRL and TensorDict One of the software hindrances in RL is the bottleneck between CPU and GPU communication majorly due to CPU-based operating environments. For this reason, we did not opt for OpenAI Gym (Brockman et al., 2016) since, although it includes some level of

[8] https://github.com/ashleve/lightning-hydra-template

parallelization, this does not happen on GPU and would thus greatly hinder performance. Kool et al. (2019) creates *ad-hoc* environments in PyTorch to handle batched data efficiently. However, it could be cumbersome to integrate into standardized routines that include `step` and `reset` functions. As we searched for a better alternative, we found that TorchRL library (Moens, 2023b), an official PyTorch project that allows for efficient batched implementations on (multiple) GPUs as well as functions akin to OpenAI Gym. We also employ the TensorDict (Moens, 2023b) to handle tensors efficiently on multiple keys (i.e. in CVRP, we can directly operate transforms on multiple keys as locations, capacities, and more). This makes our environments compatible with the models in TorchRL, which we believe could further the interest in the CO area.

PyTorch Lightning PyTorch Lightning (Falcon & The PyTorch Lightning team, 2019) is a useful tool for abstracting away the boilerplate code allowing researchers and practitioners to focus more on the core ideas and innovations. With its standardized training loop and extensive set of pre-built components, including automated checkpointing, distributed training, and logging, PyTorch Lightning accelerates development time and facilitates scalability. We employ PyTorch Lightning in RL4CO to integrate with the PyTorch ecosystem - which includes TorchRL- enabling us to leverage the rich set of tools and libraries available.

Hydra Hydra (Yadan, 2019) is a powerful open-source framework for managing complex configurations in machine learning models and other software in the form of `yaml` files. Hydra facilitates creating hierarchical configurations, making it easy to manage even very large and intricate configurations. Moreover, it integrates with command-line interfaces, allowing the execution of different configurations directly from the command line, thereby enhancing reproducibility. We found Hydra to be effective when dealing with multiple experiments, since configurations are saved both locally as `yaml` files as well as uploaded on Wandb [9].

A.3 Open Source Licenses

In this paragraph, we summarize the license of the software that we've employed in developing RL4CO. The license lists are as follows:

- PyTorch, Matplotlib: BSD license
- TorchRL, Einops, Hydra: MIT license
- Lightning: Apache-2.0 license
- Numpy, Scipy: BSD-3-Clause license

For reproducing the previous NCO research, we refer to the original implementation of AM [10], the original implementation of POMO [11], and the original implementation of SymNCO [12]. However, while faithful, our implementation considerably modifies the structure of the original implementation introducing several optimizations to single lines of codes to the overall structure. RL4CO is published under the liberal Apache-2.0 license.

A.4 Decoder with DynamicEmbedding

RL4CO provides a modular, flexible, and unified policy network design that is used for various RL algorithms to solve multiple CO problems. In this section, we provide additional discussion about the decoder structure with the dynamic embedding module that is used to solve complex routing problems involving information updates during decoding. The `DynamicEmbedding` module dynamically updates the keys and values of multi-head-attention (MHA) and softmax to reflect the 'dynamic' change of information-related unselected nodes (e.g., unvisited cities in VRPs) during decoding. To be specific, the decoder with `DynamicEmbedding` is defined as follows:

$$q_t = \texttt{ContextEmbedding}(\boldsymbol{h}, a_{t-1:0}), \tag{10}$$

[9] https://wandb.ai/
[10] https://github.com/wouterkool/attention-learn-to-route
[11] https://github.com/yd-kwon/POMO
[12] https://github.com/alstn12088/Sym-NCO

$$\boldsymbol{K}_t^g, \boldsymbol{V}_t^g, \boldsymbol{V}_t = \texttt{DynamicEmbedding}(W_k^g \boldsymbol{h}, W_v^g \boldsymbol{h}, W_v \boldsymbol{h}, a_{t-1:0}, \boldsymbol{h}, \boldsymbol{x}), \tag{11}$$

$$\bar{q}_t = \text{MHA}(q_t, \boldsymbol{K}_t^g, \boldsymbol{V}_t^g), \tag{12}$$

$$\pi(a_t) = \text{MaskedSoftmax}(\bar{q}_t \cdot \boldsymbol{V}_t, M_t), \tag{13}$$

where the dynamic embedding dynamically modulates keys and values of MHA and softmax based on the decoded results (i.e., $a_{t-1:0}$) and inputs (i.e., $\boldsymbol{x}$ and $\boldsymbol{h}$).

A.5 QUICKSTART NOTEBOOK

We showcase a quickstart Jupyter Notebook for training the Attention Model on TSP with 20 nodes that can be run in less than 2 minutes on Google Colab (Bisong & Bisong, 2019) on a free-tier GPU runtime[13].

```python
import torch
from rl4co.envs import TSPEnv
from rl4co.models.zoo.am import AttentionModel
from rl4co.utils.trainer import RL4COTrainer

# RL4CO env based on TorchRL
env = TSPEnv(num_loc=20)

# Model: default is AM with REINFORCE and greedy rollout baseline
model = AttentionModel(env,
                       baseline='rollout',
                       train_data_size=100_000,
                       val_data_size=10_000)
trainer = RL4COTrainer(max_epochs=3)

# Greedy rollouts over untrained model
device = torch.device("cuda" if torch.cuda.is_available() else "cpu")
td = env.reset(batch_size=[3]).to(device)
model = model.to(device)
out = model(td, phase="test", decode_type="greedy", return_actions=True)

# Plotting
print(f"Tour lengths: {[f'{-r.item():.2f}' for r in out['reward']]}")
for td_, actions in zip(td, out['actions'].cpu()):
    env.render(td_, actions)
```

```
Tour lengths: ['10.38', '7.69', '8.32']
```

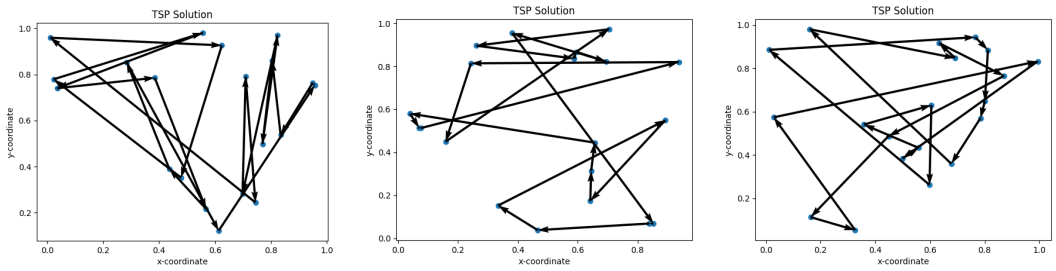

13

```
# RL4COTrainer with few epochs (wrapper around Lightning Trainer)
trainer = RL4COTrainer(
    max_epochs=3,
    accelerator="gpu",
    logger=None,
)

# Fit the model
trainer.fit(model)
```

```
INFO:
  | Name  | Type            | Params
-----------------------------------------
0 | env   | TSPEnv          | 0
1 | model | AttentionModel | 1.4 M
-----------------------------------------
1.4 M     Trainable params
0         Non-trainable params
1.4 M     Total params
5.669     Total estimated model params size (MB)

Epoch 2: [|||||||||||||||||||||||||||||||||||||||||||||||||||||||||||||] 100% 196/196
[00:44<00:00, 4.36it/s, train/reward=-4.09, train/loss=-.104, val/reward=-4.05]
```

```
# Greedy rollouts over trained model (same states as previous plot)
model = model.to(device)
out = model(td, phase="test", decode_type="greedy", return_actions=True)

# Plotting
print(f"Tour lengths: {[f'{-r.item():.2f}' for r in out['reward']]}")
for td_, actions in zip(td, out['actions'].cpu()):
    env.render(td_, actions)
```

```
Tour lengths: ['3.35', '3.51', '4.22']
```

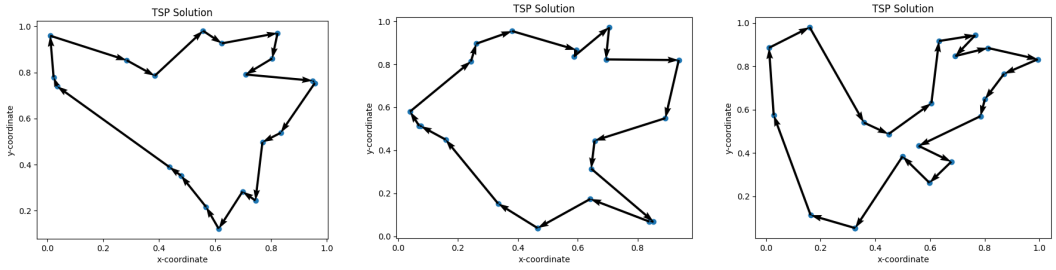

B ELECRONIC DESIGN AUTOMATION: THE DECAP PLACEMENT PROBLEM

B.1 INTRODUCTION

The optimal placement of a given number of decoupling capacitors (decaps) can significantly impact electrical performance, specifically in terms of power integrity (PI) optimization. PI optimization is crucial in modern chip design, especially with the preference for 3D stacking memory systems like high bandwidth memory (HBM), shown in Fig. B.1. One of the challenges in power supplementation is the vertical transmission of power to 3D memory, which is located at the bottom of memory chips. Consequently, the optimal placement of decaps becomes increasingly important to support the current progress in 3D chip design and high bandwidth, which is critical for meeting the high memory requirements of deep learning technology (Hwang et al., 2021).

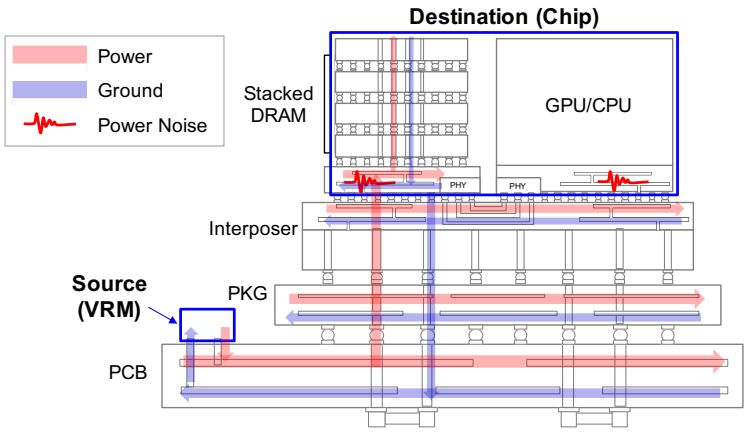

Figure B.1: An example of the power distribution network (PDN) of a high bandwidth memory (HBM) module for a high-performance AI computing system.

The optimal placement of decaps, also known as the decap placement problem (DPP), involves combinatorial optimization with a black box electrical simulator as the scoring function. Typically, this simulator is an expensive electromagnetic (EM) simulator that requires significant computational resources. To address this, we propose a fast approximated simulator that can be executed within a Python environment. While sacrificing some accuracy, our circuit-modeled simulation serves as a proxy score function. Additionally, we limit the number of simulation calls due to the high cost associated with running the real-world EM simulator.

The decap placement problem (DPP) is a highly complex task in hardware design due to two main reasons. Firstly, it involves exploring an extensive range of possibilities in a combinatorial space. Secondly, evaluating the objectives of DPP requires significant computational resources and time, making it necessary to achieve high sample efficiency. Genetic algorithm (GA) based methods have shown promise in addressing DPP because they can reduce the combinatorial space compared to exhaustive search methods (Juang et al., 2021). However, GAs still require a large number of iterations (M) for each problem as they are memoryless optimization methods. Reinforcement learning approaches have been attempted to solve DPP, and the most recently proposed DevFormer achieved the state of the art performance while achieving sample efficient in training and zero-shot inference (Kim et al., 2023).

B.2 PROBLEM SETTING

The decap placement problem (DPP) represents a sample-efficient setting of NCO, in which calculating the reward is expensive due to complex simulation, and hence the number of samples should be limited (i.e. $10,000$ samples for pretraining each model in our experiments). The DPP aims to determine the optimal locations for decaps within a given instance. This instance consists of three key components: (1) the locations of probing ports, (2) the locations of keep-out regions (where decaps cannot be placed), and (3) the available regions where decaps can be positioned as shown in

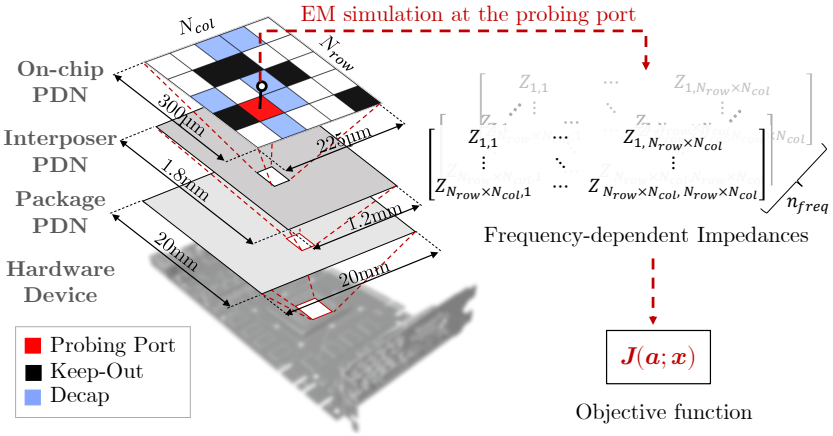

Figure B.2: Grid representation of the target on-chip PDN for the DPP problem with a single probing port.

Fig. B.2. For comprehensive details, we follow the configuration guidelines provided in (Kim et al., 2023).

Environments: DPP and mDPP In order to compare our approach with the somewhat simplistic solution to DPP presented in (Kim et al., 2023), which emphasizes placing decaps near probing ports as a good solution, we introduce multi-port DPP (mDPP) and adopt different objectives:

- *Maxsum*: the objective is to maximize the average PI among multiple probing ports
- *Maxmin*: the objective is to maximize the minimum PI among multiple probing ports

These more intricate and practical approaches add complexity to the problem, enabling us to assess the effectiveness of the proposed method in a real-world scenario. Additional details, including data generation, can be found in Appendix C.6 and Appendix C.7.

Baselines We employ two meta-heuristic baselines commonly used in hardware design as outlined in (Kim et al., 2023): random search (RS) and genetic algorithm (GA). GA has shown promise as a method for addressing the decap placement problem (DPP). In addition, we introduce DevFormer (Kim et al., 2023) (DF), an AM-variant model specifically designed for DPP. It is important to note that DevFormer is initially designed for offline training; however, in this study, we benchmark DevFormer as a sample-efficient online reinforcement learning approach.

We benchmark the DevFormer version for RL with the same embedding structure as the original in (Kim et al., 2023). We benchmark 3 variants, namely DF(PG,Critic): REINFORCE with Critic baseline, DF(PG,Rollout): REINFORCE with Rollout baseline as well as PPO. All experiments are run with the same hyperparameters as the other experiments except for the batch size set to 64, maximum number of samples set to $10,000$, and a total of only 10 epochs due to the nature of the benchmark sample efficiency.

B.3 Benchmark Results

Main benchmark Table E.2 shows the main numerical results for the task when RS, GA and DF models are trained for placing 20 decaps. While RS and GA need to take online shots to solve the problems (we restricted the number to 100), DF models can successfully predict in a zero-shot manner and outperform the classical approaches. Interestingly, the vanilla critic-based method performed the worst, while our implementation of PPO almost matched the rollout policy gradients (PG) baseline; since extensive hyperparameter tuning was not performed, we expect PPO could outperform the rollout baseline given it requires fewer samples. Fig. B.3 shows example renderings of the solved environment.

Table B.1: Performance of different methods on the mDPP benchmark

Method	# Shots	*Score* ↑ maxsum	maxmin
Online Test Time Search			
Random Search	100	11.55	10.63
Genetic Algorithm	100	11.93	11.07
RL Pretraining & Zero Shot Inference			
DF-(PG,Critic)	0	10.89 ± 0.63	9.51 ± 0.68
DF-(PPO)	0	12.16 ± 0.03	11.17 ± 0.11
DF-(PG,Rollout)	0	12.21 ± 0.01	11.26 ± 0.03

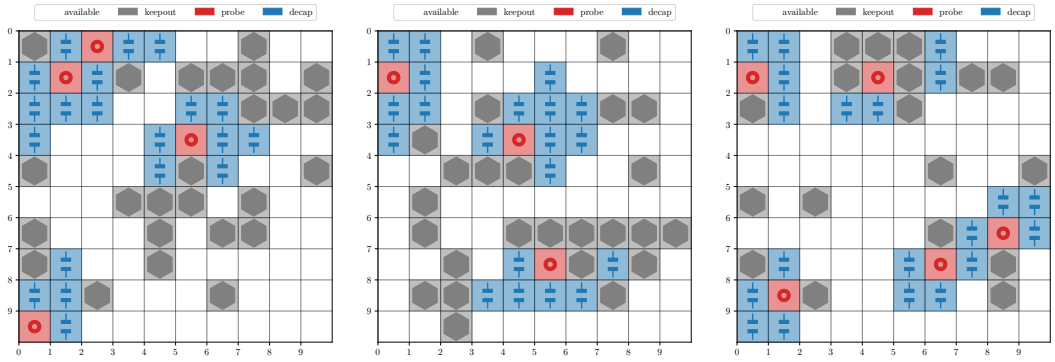

Figure B.3: Renders of the environment with *maxmin* objective solved by DF-(PG,Rollout). The model successfully learned one main heuristic for DPP problems, which is that optimal placement is generally close to probing ports.

Generalization to different number of decaps In hardware design, the number of components is one major contribution to cost; ideally, one would want to use the least number of components possible with the best performance. In the DPP, increasing the number of decaps *generally* improves the performance at a greater cost, hence Pareto-efficient models are essential to identify. Fig. B.4 shows the performance of DF models trained on 20 decaps against the baselines. DF models PPO and PG-rollout can successfully generalize and are also Pareto-efficient with fewer decaps, important in practice for cost and material saving.

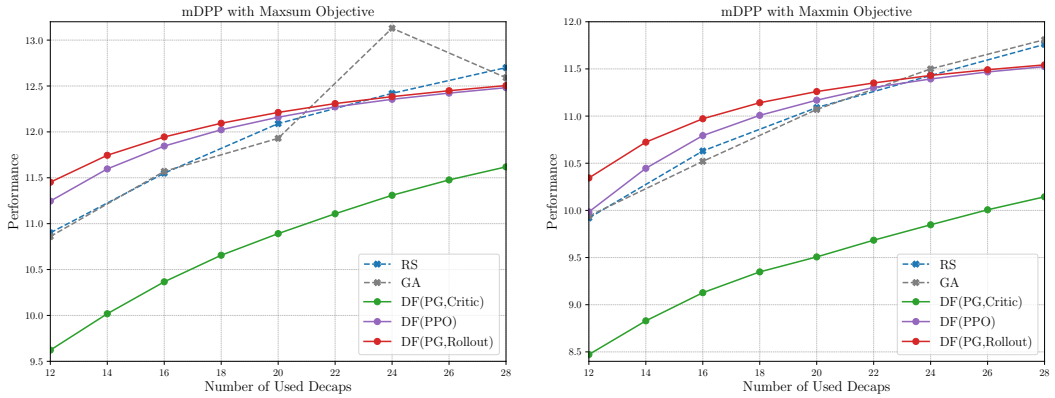

Figure B.4: Performance vs number of used decaps for mDPP with *maxsum* objective [Left] and *maxmin* objective [Right].

C ENVIRONMENTS

In this section, we discuss further details of environment implementation. As Kool et al. (2019) environment implementation de-facto standard of implementation, RL4CO also aims to reproduce the same environment settings along with generating the same data.

Common instance generation details Following the standard protocol of NCO, we randomly sample node coordinates from the 2D unit square (i.e., $[0, 1]^2$). When generating the training data, we regulate the randomness by setting the random seed to 1234. Conversely, when generating 10,000 validation instances, we use random seed 4321. For the creation of the testing 10,000 instances, we use the random seed 1234. All protocols, including seed selection, align with the practices outlined by Kool et al. (2019).

C.1 TRAVELING SALESMAN PROBLEM (TSP)

The Traveling Salesman Problem (TSP) is a fundamental routing problem that aims to find the Hamiltonian cycle of minimum length. While the original TSP formulation employs mixed-integer linear programming (MILP), to integrate TSP into autoregressive solution decoding (i.e., the construction process), we reinterpret the solution-finding process as sequential node selection in line with Kool et al. (2019). In each step of node selection, we preclude the selection of nodes already picked in previous rounds. This procedure ensures the feasibility of constructed solutions and also allows for the potential construction of an optimal solution for any TSP instance.

C.2 CAPACITATED VEHICLE ROUTING PROBLEM (CVRP)

The Capacitated Vehicle Routing Problem (CVRP) is a popular extension of TSP, applicable to a variety of real-world logistics/routing problems (e.g., delivery services). In CVRP, each node has its own demand, and each vehicle has a specific capacity. A vehicle can "tour" until the total demand does not exceed its capacity. The vehicle returns to the depot - a unique type of node - and releases all demand, then embarks on another tour from the depot until all nodes have been visited. Similar to TSP, the original CVRP formulation utilizes MILP. However, by applying a similar logic to that of the TSP environment, we can reformulate CVRP as a sequential node selection problem, taking into account demands and capacity.

Additional generation details To generate demand, we randomly sample integers between 1 and 10. Without loss of generality, we fix the capacity of the vehicle at 1.0. Instead, we normalize demand by multiplying it by a constant that varies according to the size of the CVRP. The specific constant can be found in our implementation.

C.3 ORIENTEERING PROBLEM (OP)

The Orienteering Problem (OP) is a variant of TSP. In OP, each node (i.e., city) is assigned a prize. The objective of OP is to find a tour, starting and ending at the depot, that maximizes the total prize collected from visited cities, while abiding by a maximum tour length constraint. Like the previous problems, the original formulation utilizes MILP. However, OP can also be framed as a sequential decision-making problem by enforcing the "return to depot" action when no cities are visitable due to the maximal tour length constraint.

Additional generation details To generate the prize, we use the prize distribution proposed in Fischetti et al. (1998), particularly the distribution that allocates larger prizes to nodes further from the depot.

C.4 PRIZE COLLECTING TSP (PCTSP)

In the Prize Collecting TSP (PCTSP), each node is assigned both a prize and a penalty. The objective is to accumulate a minimum total prize while minimizing the combined length of the tour and the penalties for unvisited nodes. By making a minor adjustment to PCTSP, it becomes applicable

for solving different subproblems that arise in routing problems when using Branch-Price-and-Cut algorithms.

C.5 Pickup and Delivery Problem (PDP)

The Pickup and Delivery Problem (PDP) is an extension of TSP. In PDP, a pickup node has its own designated delivery node. The delivery node can be visited only when its paired pickup node is already visited, so-called, precedence constraints. The objective of PDP is to find a complete tour with a minimal tour length while starting from the depot node and satisfying the precedence constraints. We assume the 'stacking' is allowed, where the traveling agent can visit multiple pickups prior to visiting the paired deliveries.

Additional generation details To generate the positions of the depot, pickups, and deliveries, we sample the node coordinates from the 2D unit square.

C.6 Decap Placement Problem (DPP)

The decap placement problem (DPP) is an electronic design automation problem (EDA) in which the goal is to maximize the performance with a limited number of the decoupling capacitor (decap) placements on a hardware board characterized by asymmetric properties, measured via a probing port. The decaps cannot be placed on the location of the probing port or in keep-out regions (which represent other hardware components). The full problem description is provided in Appendix B.

Instance generation details We use the same data for simulating the hardware board as Kim et al. (2023). We randomly select one probing port and a number between 1 and 50 keep-out regions sampled from a uniform distribution for generating instances. As in the routing benchmarks, we select seed 1234 for testing the 100 instances.

C.7 Multi-Port Decap Placement Problem (mDPP)

The multi-port decap placement problem (mDPP) is a generalization of DPP from Appendix C.6 in which measurements from multiple probing ports are performed. The objective function can be either the mean of the reward from the probing ports (*maxsum*) or the minimum between them (*maxmin*).The full problem description is provided in Appendix B.

Instance generation details The generation details are the same as DPP, except for the probing port. A number between 2 and 5 probing ports is sampled from a uniform distribution and probing ports are randomly placed on the board as the other components.

C.8 Additional Environments

We also include in the RL4CO library additional environments on which we did not benchmark models for the time being due to time and resource constraints: the Pickup and Delivery Problem and its multi-agent version (PDP and mPDP), the multiple Traveling Salesman Problem (mTSP), as well as asymmetric CO environments Asymmetric Traveling Salesman Problem (ATSP) and Flexible Flow Shop Problem (FFSP). We include also the Stochastic variant of PCTSP (SPCTSP) and a variation of the CVRP that allows for split deliveries to be considered, namely the Split Delivery Vehicle Routing Problem (SDVRP) - we show an example notebook on the latter under the `notebook/` folder of the library. Given both near and longer-term plans for the library and the RL4CO community, we expect to add several more variations as well as new environments in the future.

D EXPERIMENTAL DETAILS

D.1 HARDWARE

Experiments were carried out on a machine equipped with two AMD EPYC 7542 32-CORE PROCESSOR CPU with 64 threads and four NVIDIA RTX A6000 graphic cards with 48 GB of VRAM.

D.2 SOFTWARE

Software-wise, we used `Python 3.10` and the latest PyTorch 2.0 (Paszke et al., 2019) (during development, we used beta wheels as well as manually installed version of FlashAttention (Dao et al., 2022; Dao, 2023)), most notably due to the native implementation of `scaled_dot_product_attention`. Given that most models in RL constructive methods for CO generally use attention for encoding states, FlashAttention has some boost on the performance (between 5% and 20% saved time depending on the problem size) when training is subject to mixed-precision training, which we do for all experiments. During decoding, the FlashAttention routine is not called since, at the time of writing, it does not support maskings other than causal; this could further boost performance compared to older implementations. Refer to Appendix A.2 for additional details regarding notable software choices of our library, namely TorchRL, PyTorch Lightning and Hydra.

D.3 COMMON HYPERPARAMETERS

Common hyperparameters can be found in the `config/` folder from the RL4CO library, which can be conveniently loaded by Hydra. We provide yaml-like configuration files below, divided by experiments in Listing 1.

D.4 CLASSICAL SOLVERS

We report performance in terms of optimality gaps compared with the best-known solutions we obtain across methods. For the TSP, we use the Gurobi results (Gurobi Optimization, 2021) results from (Kool et al., 2019) and Concorde (Mulder & Wunsch II, 2003; David Applegate & Cook, 2023). For CVRP, we used HGS (Vidal, 2022) as a baseline, which is shown to be superior to alternatives. For the OP, we report the results from Compass (Golden et al., 1987). As more general-purpose solvers for routing problems, we also report LKH3 Helsgaun (2017) and Google OR Tools (Perron & Furnon, 2023).

D.5 MAIN TABLES

We run all models to try and match as much as possible the original implementation details. In particular, we run all models for $250,000$ gradient steps with the same Adam (Kingma & Ba, 2014) optimizer with a learning rate of 10^{-4} and 0 weight decay. For POMO, we match the original implementation details of weight decay as 10^{-6}. For POMO, the number of multistarts is the same as the number of possible initial locations in the environment (for instance, for TSP50, 50 starts are considered). In the case of Sym-NCO, we use 10 as augmentation for the shared baseline; we match the number of effective samples of AM-XL to the ones of Sym-NCO to demonstrate the differences between models.

Common configuration

```yaml
# RL Model configuration (policy+baseline)
model:
    policy:
        encoder:
            type: GraphAttentionEncoder
            num_heads: 8
            num_layers: 3 # POMO uses 6
            normalization: "batch" # POMO uses "instance"
            hidden_dim: 512
            embedding_dim: 128
        decoder:

            num_heads: 8
            embedding_dim: 128
            use_graph_context: True # POMO does not use it
            tanh_clipping: 10.0
            mask_inner: True
            mask_logits: True
            normalize: True
            softmax_temp: 1.0
    baseline:
        "rollout" # default baseline

# Training configuration

train:
    optimizer:
        type: Adam
        learning_rate: 1e-4
        weight_decay: 0 # POMO uses 1e-6
    scheduler:
        type: MultiStepLR # original AM implementation does not use
        ↪  this
        step_size: [80, 95]
        gamma: 0.1
        scheduler_interval: epoch
    gradient_clip_val: 1.0

    max_epochs: 100 # we set AM-XL to 500
    precision: "16-mixed" # allows for FlashAttention
    strategy: DDPStrategy # efficient for multiple GPUs

```

Listing 1: Common configuration for RL model (policy + baseline) and training. Some differences are highlighted, such as the POMO implementation-level ones, and are provided as comments.

The number of epochs for all models is 100, except for AM-XL (500). We also employ learning rate scheduling, in particular, `MultiStepLR` [14] with $\gamma = 0.1$ on epoch 80 and 95; for AM-XL, this applies on epoch 480 and 495.

D.6 Sample Efficiency Experiments

We keep the same hyperparameters as Appendix D.5, except for the number of epochs and scheduling. We consider 5 independent runs that match the number of samples *per step* (i.e., the batch size is exactly the same for all models after considering techniques such as the multistart and symmetric baselines). For AM Rollout, we employ half the batch size of other models since it requires double the number of evaluations due to its baseline.

[14] https://pytorch.org/docs/stable/generated/torch.optim.lr_scheduler.MultiStepLR

D.7 SEARCH METHODS EXPERIMENTS

For these experiments, we employ the same models trained in the in-distribution benchmark on 50 nodes. For Active Search (AS), we run 200 iterations for each instance and an augmentation size of 8. The Adam optimizer is used with learning rate of 2.6×10^{-4} and weight decay of 10^{-6}. For Efficient Active Search, we benchmark EAS-Lay (with an added layer during the single-head computation, `LogitAttention` in our code) with the original hyperparameters proposed by Hottung et al. (2022). The learning rate is set to 0.0041 and weight decay to 10^{-6}. The search is restricted to 200 iterations with dihedral augmentation of 8 as well as imitation learning weight $\lambda = 0.013$.

Testing is performed on 100 instances on both TSP and CVRP for $N \in [200, 500, 1000]$, generated with the usual random seed for testing 1234.

D.8 PPO IMPLEMENTATION DETAILS

We also implemented PPO, the Attention Model trained with Proximal Policy Optimization (Schulman et al., 2017), which was not considered in previous works. We use the same critic network as the critic network for the critic REINFORCE baseline and perform training with the same settings as the AM-Critic based on REINFORCE.

Contrary to the common interpretation that views the solution generation process of CO problems (i.e., Eq. (1)) as a Markov Decision Process (MDP), where each decoding step corresponds to a state transition, we view it as a single-stage problem with an auto-regressive policy construction structure. Following this interpretation, the iterations in the decoding steps do not coincide with MDP's time step updates.

This interpretation requires some modifications to PPO, especially in computing the training labels of the value network (i.e., the value of the value function) to train NCO solvers. Since we have only one stage, our value function predicts the expected cost given the policy from the given problem instance. It is noteworthy that the problem is single-staged; hence, the Generalized Advantage Estimator (GAE) is not applicable, as GAE computes the values in the multi-stage setting. We found that recent fine-tuning of a large language model (Ouyang et al., 2022) carried out by PPO also interprets the decoding scheme as a single-state problem and hence does not apply GAE.

As for other hyperparameters, we set the number of epochs to 2, mini-batch size to 512, clip range to 0.2, and entropy coefficient $c_2 = 0.01$. Interestingly, we found that normalizing the advantage as done in the Stable Baselines PPO2 implementation[15] slightly hurt performance, so we set the normalize advantage parameter to `False`. We suspect this is because the NCO solvers are trained on *multiple* problem instances, unlike the other RL applications that aim to learn a policy for a single MDP.

[15] https://stable-baselines.readthedocs.io/en/master/modules/ppo2.html

E ADDITIONAL EXPERIMENTS

E.1 TRAINING ON SMALLER SIZES

In this section, we provide additional benchmark results on smaller instances, where the problems have 20 nodes. These include Table E.1[16], Fig. E.1 and Fig. E.2. The general trends of the results are similar to the ones observed from the problems with 50 nodes.

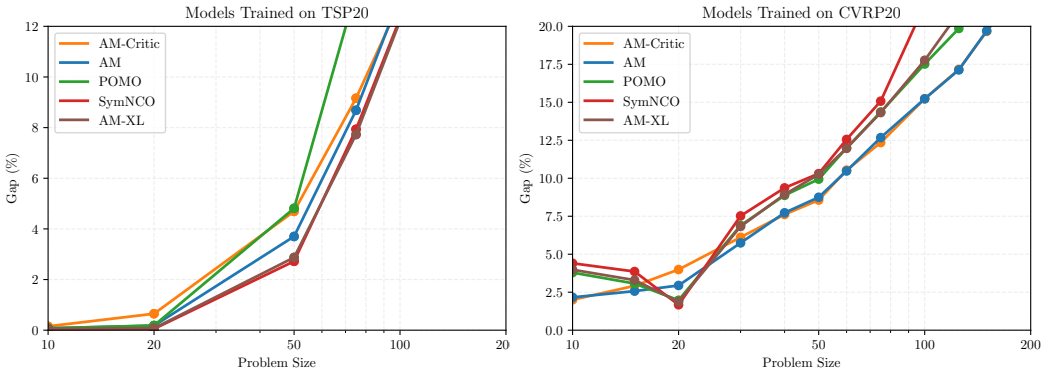

Figure E.1: Out-of-distribution generalization results. Models tend to perform better on problem of the same size of those seen during training.

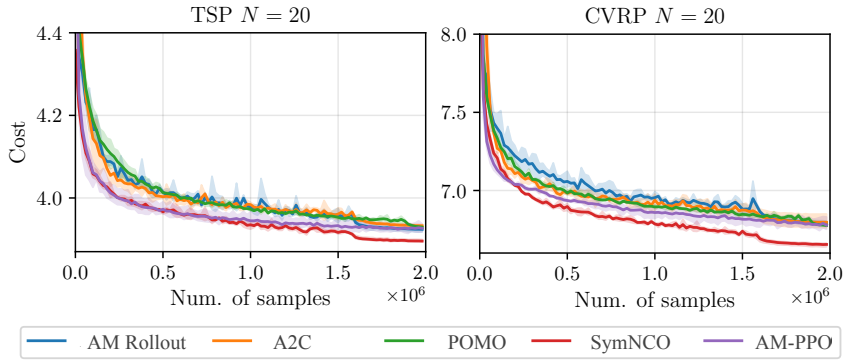

Figure E.2: Additional sample efficiency results for smaller problems with 20 nodes. Interestingly, SymNCO can outperform baselines even in TSP in terms of sample efficiency.

E.2 FLOATING POINT PRECISION AND FLASH ATTENTION

RL4CO supports multiple device types as well as floating point precisions by leveraging PyTorch Lightning (Falcon & The PyTorch Lightning team, 2019).

As Appendix E.2 shows mixed-precision training can successfully reduce computational costs both in terms of runtime and especially with memory usage. Moreover, we designed our model to natively support FlashAttention (Dao et al., 2022; Dao, 2023) from both PyTorch 2.0 and the original FlashAttention repository [17].

As shown in Fig. E.3, different implementations can make a difference, especially with large problem sizes. It should be noted that while more scalable, FlashAttention at the moment is restricted to no or causal masks only. Therefore, usage in the masked attention decoding scheme is not possible

[16] We take the result for CPLEX from HAM (Li et al., 2021a).
[17] Available at https://github.com/Dao-AILab/flash-attention.

Table E.1: In-distribution results for model trained on 20 nodes.

Method	TSP			CVRP			OP			PCTSP			PDP		
	Cost ↓	Gap	Time	Cost ↓	Gap	Time	Prize ↑	Gap	Time	Cost ↓	Gap	Time	Cost ↓	Gap	Time
Classical Solvers															
Gurobi†	3.84	0.00%	7s	–	–	–	–	–	–	–	–	–	–	–	–
Concorde	3.84	0.00%	1m	–	–	–	5.39	0.00%	16m	3.13	0.00%	2m	–	–	–
HGS	–	–	–	6.13	0.00%	4h	–	–	–	–	–	–	–	–	–
Compass	–	–	–	–	–	–	–	–	–	–	–	–	–	–	–
LKH3	3.84	0.00%	15s	6.14	0.16%	5h	–	–	–	–	–	–	–	–	–
OR Tools	3.85	0.37%	1m	–	–	–	–	–	–	3.13	0.00%	5h	4.70	3.16%	(<1s)
CPLEX	–	–	–	–	–	–	–	–	–	–	–	–	4.56	0.00%	7m23s
Greedy One Shot Evaluation															
A2C	3.86	0.64%	(<1s)	6.46	5.00%	(<1s)	5.01	6.70%	(<1s)	3.36	7.35%	(<1s)	5.50	20.61%	(<1s)
AM	3.84	0.19%	(<1s)	6.39	3.92%	(<1s)	5.20	3.17%	(<1s)	3.17	1.28%	(<1s)	4.82	5.70%	(<1s)
POMO	3.84	0.18%	(<1s)	6.33	3.00%	(<1s)	4.69	12.69%	(<1s)	3.41	8.95%	(<1s)	4.85	6.36%	(<1s)
Sym-NCO	3.84	0.05%	(<1s)	6.30	2.58%	(<1s)	5.30	1.37%	(<1s)	3.15	0.64%	(<1s)	4.70	3.07%	(<1s)
AM-XL	3.84	0.07%	(<1s)	6.31	2.81%	(<1s)	5.25	2.23%	(<1s)	3.17	1.26%	(<1s)	4.71	3.29%	(<1s)
Sampling with width $M = 1280$															
A2C	3.84	0.15%	20s	6.26	2.08%	24s	5.12	4.66%	22s	3.28	4.79%	23s	5.06	10.96%	23s
AM	3.84	0.04%	20s	6.24	1.78%	24s	5.30	1.30%	22s	3.15	0.78%	23s	4.66	2.19%	23s
POMO	3.84	0.02%	36s	6.20	1.06%	40s	4.90	8.83%	37s	3.33	6.39%	39s	4.68	2.63%	39s
Sym-NCO	3.84	0.01%	36s	6.22	1.44%	40s	5.34	0.59%	37s	3.14	0.35%	39s	4.64	1.75%	39s
AM-XL	3.84	0.02%	36s	6.22	1.46%	40s	5.32	0.93%	37s	3.15	0.56%	39s	4.64	1.75%	39s
Greedy Multistart (N)															
A2C	3.85	0.36%	(<1s)	6.33	3.04%	3s	5.06	5.77%	2s	3.30	5.18%	2s	5.18	13.60%	23s
AM	3.84	0.12%	(<1s)	6.28	2.27%	3s	5.24	2.42%	2s	3.16	4.67%	2s	4.67	2.41%	23s
POMO	3.84	0.05%	(<1s)	6.21	1.27%	4s	4.76	11.32%	3s	3.35	4.65%	4s	4.66	2.19%	42s
Sym-NCO	3.84	0.03%	(<1s)	6.22	1.48%	4s	5.32	0.87%	3s	3.15	4.69%	4s	4.69	2.85%	42s
AM-XL	3.84	0.05%	(<1s)	6.22	1.38%	4s	5.29	1.49%	3s	3.15	4.6%	4s	4.65	1.97%	42s
Greedy with Augmentation (1280)															
A2C	3.84	0.01%	20s	6.22	1.35%	24s	5.04	6.10%	22s	3.33	6.39%	23s	4.88	7.02%	23s
AM	3.84	0.00%	20s	6.20	1.07%	24s	5.25	2.25%	22s	3.16	0.96%	23s	4.63	1.54%	23s
POMO	3.84	0.00%	36s	6.18	0.84%	45s	4.85	9.76%	38s	3.37	7.55%	42s	4.62	1.32%	42s
Sym-NCO	3.84	0.00%	36s	6.17	0.71%	45s	5.33	0.77%	38s	3.15	0.63%	42s	4.61	0.95%	42s
AM-XL	3.84	0.00%	36s	6.17	0.68%	45s	5.30	1.30%	38s	3.15	0.68%	42s	4.61	0.96%	42s
Greedy Multistart with Augmentation $(N \times 16)$															
A2C	3.84	0.01%	9s	6.20	1.12%	48s	5.20	3.17%	32s	3.28	4.95%	25s	4.87	6.80%	23s
AM	3.84	0.00%	9s	6.18	0.78%	48s	5.34	0.56%	32s	3.14	0.32%	25s	4.63	1.52%	23s
POMO	3.84	0.00%	13s	6.16	0.50%	1m	5.09	5.29%	45s	3.35	6.95%	38s	4.61	1.10%	42s
Sym-NCO	3.84	0.00%	13s	6.17	0.61%	1m	5.35	0.39%	45s	3.14	0.24%	38s	4.60	0.89%	42s
AM-XL	3.84	0.00%	13s	6.16	0.44%	1m	5.35	0.46%	45s	3.14	0.28%	38s	4.60	0.87%	42s

Table E.2: Running time and memory usage of the AM model trained using FP32 and FP16 mixed precision (FP16-mix), evaluated over 5 epochs with a training size of 10,000 in the CVPR20, CVPR50, and CVPR100.

Problem	Precision	Running time [s]	Memory usage [GiB]
CVRP20	FP32	6.33 ± 0.26	1.41 ± 0.04
	FP16-mix	5.89 ± 0.07	0.84 ± 0.01
CVRP50	FP32	13.58 ± 0.12	4.79 ± 0.40
	FP16-mix	11.68 ± 0.30	2.30 ± 0.25
CVRP100	FP32	35.09 ± 0.71	13.47 ± 0.63
	FP16-mix	25.11 ± 0.66	8.14 ± 0.82

for the time being, although it could be even more impactful due to the auto-regressive nature of our encoder-decoder scheme [18].

[18] A recent work, Pagliardini et al. (2023), may be useful in extending FlashAttention to other masking patterns.

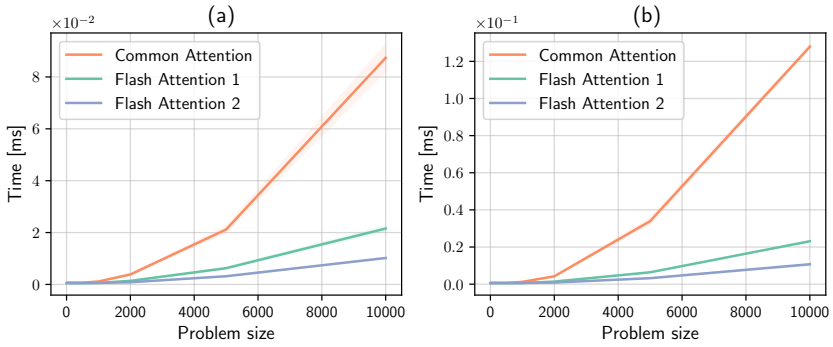

Figure E.3: Running time of the graph attention encoder from the Attention Model, equipped with a standard attention layer, FlashAttention1, and FlashAttention2, across different problem sizes for both (a) the TSP and (b) the CVRP environments.

F TSP AND CVRP PUBLIC BENCHMARK

In this section, we evaluate the NCO models trained on randomly generated uniform datasets with 20 and 50 nodes against public benchmark datasets. For the Traveling Salesman Problem (TSP), we evaluate the models using instances from TSPLib (Reinelt, 1991) with fewer than 250 nodes. For the Capacitated Vehicle Routing Problem (CVRP), we evaluate the models using instances from Set A, B, E, F, and M from CVRPLib (Ivan). The optimal or best-known solutions (BKS) of evaluated TSP and CVRP instances are taken from (Reinelt, 1991) and (Ivan). Note that we observed that NCO models with `Augmentation` discovered the solution with a lower cost than the reported BKS for B-n51-k7 of CVRPLib.

Evaluation results Similar to the random instance evaluations, we tested the models with different decoding schemes, including `Greedy`, `Sampling`, `Multistart`, and `Augmentation`. We provide a shortcut link to each combination of results in Table F.1. From the results, we once again confirmed that `Augmentation` generally outperforms the other sampling techniques, with a similar (or smaller) number of sample evaluations and the network forward, similar to the random instance benchmarks.

Table F.1: Table of TSPLib and CVRPLib results

Dataset	Trained on	Decoding scheme			
		`Greedy`	`Sampling`	`Multistart`	`Augmentation`
TSPLib	20	Table F.2	Table F.3	Table F.4	Table F.5
	50	Table F.6	Table F.7	Table F.8	Table F.9
CVRPLib	20	Table F.10	Table F.11	Table F.12	Table F.13
	50	Table F.14	Table F.15	Table F.16	Table F.17

Visualized results Here we share the tours (i.e., solutions) of the CVRP instances where NCO models tend to have worse and better performances compared to the optimal (or BKS) solutions. We found that NCO solvers have a tendency that NCO solvers generalize quite well to the variation of size with proper scaling on the coordinates of city positions by inspecting the A sets in CVRP. (See Fig. F.3.) However, they often show drastic performance degradation in the instances that are not generated from uniform (or close to) distribution by inspecting the non-A datasets (e.g., the sets B and F) as shown in Figs. F.4 and F.5.

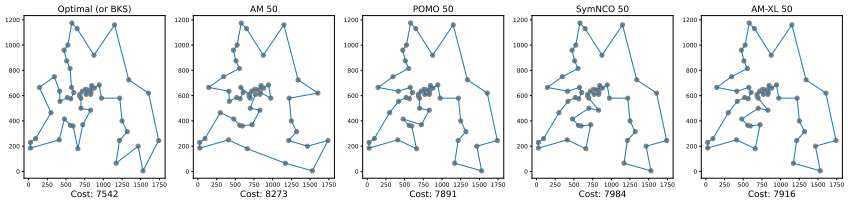

(a) `Greedy` decoding

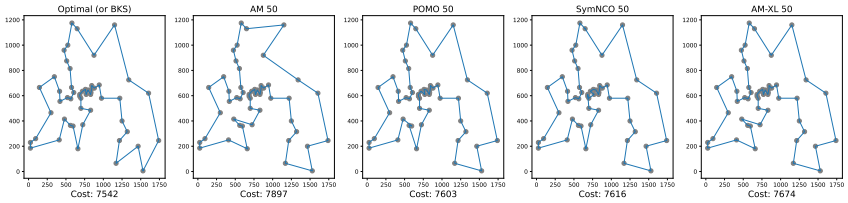

(b) `Augmentation` decoding

Figure F.1: (TSPLib) Solutions of Berlin52 instance

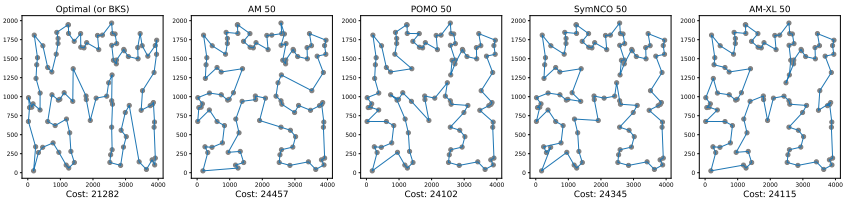

(a) `Greedy` decoding

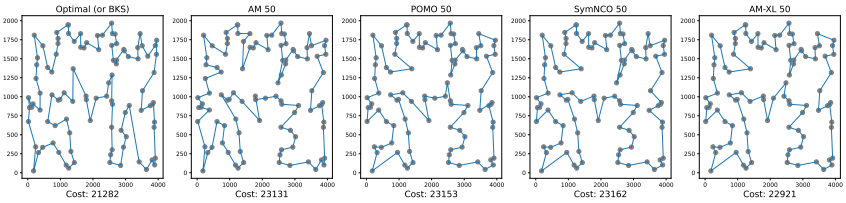

(b) `Augmentation` decoding

Figure F.2: (TSPLib) Solutions of KroA100 instance

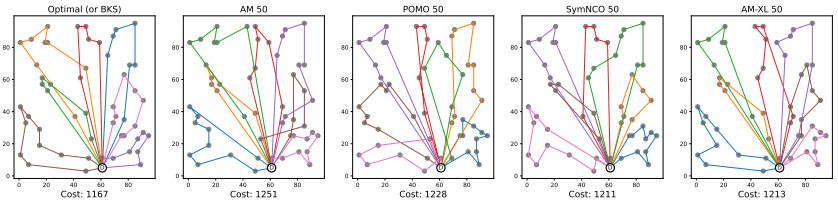

(a) `Greedy` decoding

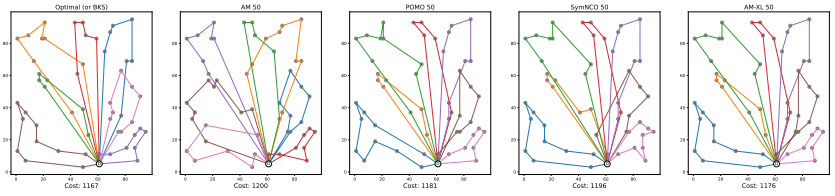

(b) `Augmentation` decoding

Figure F.3: (CVRPLib) Solutions of A-n54-k7 instance

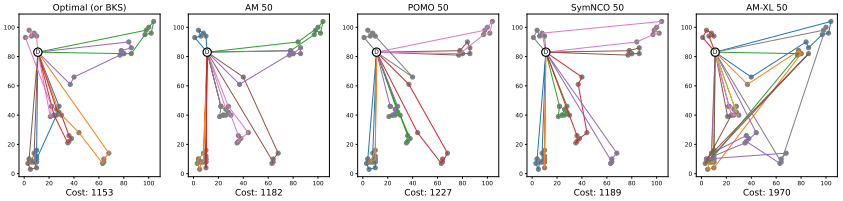

(a) `Greedy` decoding

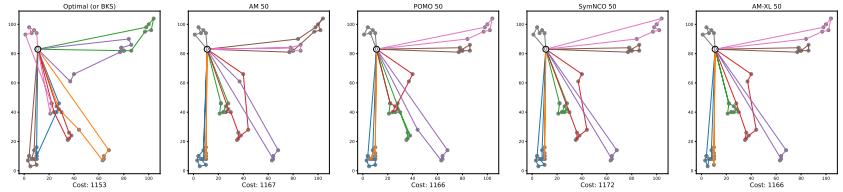

(b) `Augmentation` decoding

Figure F.4: (CVRPLib) Solutions of B-n57-k7 instance

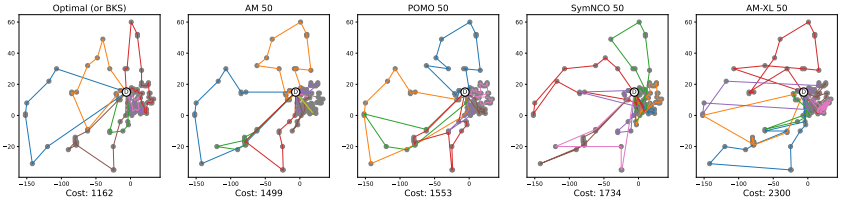

(a) `Greedy` decoding

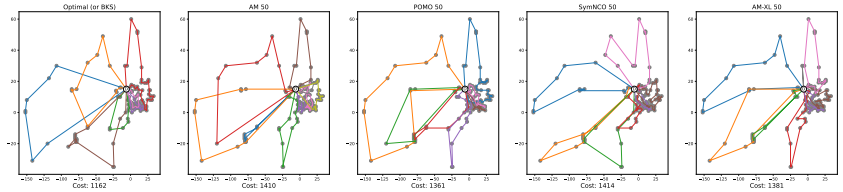

(b) `Augmentation` decoding

Figure F.5: (CVRPLib) Solutions of F-n135-k7 instance

Table F.2: TSPLib results. The models are trained on TSP20. Greedy decoding is used.

Instance	Opt. (BKS)	AM		POMO		SymNCO		AM-XL	
		Cost	Gap ↓	Cost	Gap ↓	Cost	Gap ↓	Cost	Gap ↓
eil51	426	458	6.99 %	488	12.70 %	462	7.79 %	455	6.37 %
berlin52	7542	8623	12.54 %	8757	13.87 %	8518	11.46 %	8621	12.52 %
st70	675	718	5.99 %	736	8.29 %	744	9.27 %	733	7.91 %
eil76	538	602	10.63 %	606	11.22 %	623	13.64 %	618	12.94 %
pr76	108159	116536	7.19 %	123427	12.37 %	119133	9.21 %	115082	6.02 %
rat99	1211	1764	31.35 %	1648	26.52 %	1593	23.98 %	1728	29.92 %
kroA100	21282	24999	14.87 %	28827	26.17 %	26330	19.17 %	26826	20.67 %
kroB100	22141	27325	18.97 %	32980	32.87 %	28256	21.64 %	26209	15.52 %
kroC100	20749	24908	16.70 %	25392	18.29 %	26762	22.47 %	26980	23.09 %
kroD100	21294	25742	17.28 %	27993	23.93 %	25152	15.34 %	25180	15.43 %
kroE100	22068	25985	15.07 %	26754	17.52 %	24751	10.84 %	25494	13.44 %
rd100	7910	9324	15.17 %	9011	12.22 %	9121	13.28 %	9096	13.04 %
eil101	629	752	16.36 %	769	18.21 %	733	14.19 %	732	14.07 %
lin105	14379	17540	18.02 %	17681	18.68 %	17448	17.59 %	17209	16.44 %
pr124	59030	63859	7.56 %	68615	13.97 %	65788	10.27 %	68607	13.96 %
bier127	118282	141651	16.50 %	167812	29.52 %	145686	18.81 %	139922	15.47 %
ch130	6110	6993	12.63 %	8114	24.70 %	7122	14.21 %	7367	17.06 %
pr136	96772	116722	17.09 %	117786	17.84 %	114860	15.75 %	112008	13.60 %
pr144	58537	64888	9.79 %	65724	10.94 %	66244	11.63 %	66012	11.32 %
kroA150	26524	34041	22.08 %	39355	32.60 %	34499	23.12 %	35034	24.29 %
kroB150	26130	34394	24.03 %	40379	35.29 %	35975	27.37 %	34700	24.70 %
pr152	73682	85034	13.35 %	103086	28.52 %	85237	13.56 %	87594	15.88 %
u159	42080	52067	19.18 %	67675	37.82 %	53603	21.50 %	52161	19.33 %
rat195	2323	3761	38.23 %	3492	33.48 %	3431	32.29 %	3533	34.25 %
kroA200	29368	38338	23.40 %	45189	35.01 %	41007	28.38 %	38696	24.11 %
ts225	126643	170904	25.90 %	175644	27.90 %	165864	23.65 %	165968	23.69 %
tsp225	3919	5514	28.93 %	5490	28.62 %	5251	25.37 %	5279	25.76 %
pr226	80369	96413	16.64 %	117181	31.41 %	94562	15.01 %	88617	9.31 %
Avg. Gap	0.00 %	17.23%		22.87%		17.53%		17.15%	

Table F.3: TSPLib results. The models are trained on TSP20. Sampling decoding (100 with temperature $\tau = 0.05$) is used.

Instance	Opt. (BKS)	AM		POMO		SymNCO		AM-XL	
		Cost	Gap ↓	Cost	Gap ↓	Cost	Gap ↓	Cost	Gap ↓
eil51	426	452	5.75 %	455	6.37 %	453	5.96 %	452	5.75 %
berlin52	7542	8623	12.54 %	8659	12.90 %	8503	11.30 %	8326	9.42 %
st70	675	714	5.46 %	715	5.59 %	722	6.51 %	733	7.91 %
eil76	538	589	8.66 %	593	9.27 %	594	9.43 %	580	7.24 %
pr76	108159	113356	4.58 %	121733	11.15 %	113680	4.86 %	114846	5.82 %
rat99	1211	1683	28.05 %	1556	22.17 %	1545	21.62 %	1592	23.93 %
kroA100	21282	24614	13.54 %	27074	21.39 %	26549	19.84 %	25947	17.98 %
kroB100	22141	25083	11.73 %	28736	22.95 %	26982	17.94 %	24498	9.62 %
kroC100	20749	24330	14.72 %	24666	15.88 %	25006	17.02 %	24432	15.07 %
kroD100	21294	24307	12.40 %	25464	16.38 %	24590	13.40 %	24602	13.45 %
kroE100	22068	25292	12.75 %	26232	15.87 %	24879	11.30 %	24610	10.33 %
rd100	7910	9028	12.38 %	8604	8.07 %	8990	12.01 %	8754	9.64 %
eil101	629	706	10.91 %	732	14.07 %	715	12.03 %	710	11.41 %
lin105	14379	17194	16.37 %	16953	15.18 %	16629	13.53 %	17081	15.82 %
pr124	59030	66264	10.92 %	71454	17.39 %	68208	13.46 %	69766	15.39 %
bier127	118282	135364	12.62 %	146716	19.38 %	144157	17.95 %	140514	15.82 %
ch130	6110	6897	11.41 %	7225	15.43 %	6940	11.96 %	6945	12.02 %
pr136	96772	111847	13.48 %	114434	15.43 %	112828	14.23 %	111362	13.10 %
pr144	58537	67643	13.46 %	68830	14.95 %	72190	18.91 %	70068	16.46 %
kroA150	26524	33358	20.49 %	34358	22.80 %	34281	22.63 %	33881	21.71 %
kroB150	26130	31668	17.49 %	35325	26.03 %	34494	24.25 %	33365	21.68 %
pr152	73682	86191	14.51 %	89573	17.74 %	89469	17.65 %	88763	16.99 %
u159	42080	52987	20.58 %	58999	28.68 %	54263	22.45 %	52393	19.68 %
rat195	2323	3558	34.71 %	3472	33.09 %	3329	30.22 %	3557	34.69 %
kroA200	29368	37013	20.65 %	43916	33.13 %	41634	29.46 %	39579	25.80 %
ts225	126643	175030	27.64 %	179713	29.53 %	182349	30.55 %	176018	28.05 %
tsp225	3919	5390	27.29 %	5686	31.08 %	5510	28.87 %	5389	27.28 %
pr226	80369	100274	19.85 %	108547	25.96 %	106235	24.35 %	105694	23.96 %
Avg. Gap	0.00 %	15.53%		18.85%		17.27%		16.29%	

Table F.4: TSPLib results. The models are trained on TSP20. Greedy multi-start decoding is used.

Instance	Opt. (BKS)	AM		POMO		SymNCO		AM-XL	
		Cost	Gap ↓	Cost	Gap ↓	Cost	Gap ↓	Cost	Gap ↓
eil51	426	458	6.99 %	449	5.12 %	453	5.96 %	454	6.17 %
berlin52	7542	8623	12.54 %	8075	6.60 %	8251	8.59 %	8419	10.42 %
st70	675	713	5.33 %	711	5.06 %	735	8.16 %	716	5.73 %
eil76	538	602	10.63 %	606	11.22 %	601	10.48 %	600	10.33 %
pr76	108159	113356	4.58 %	113227	4.48 %	118432	8.67 %	113647	4.83 %
rat99	1211	1680	27.92 %	1556	22.17 %	1559	22.32 %	1647	26.47 %
kroA100	21282	23771	10.47 %	26118	18.52 %	25840	17.64 %	26826	20.67 %
kroB100	22141	25721	13.92 %	27440	19.31 %	26081	15.11 %	25275	12.40 %
kroC100	20749	24377	14.88 %	23883	13.12 %	25633	19.05 %	24224	14.35 %
kroD100	21294	25429	16.26 %	24914	14.53 %	23878	10.82 %	25047	14.98 %
kroE100	22068	25354	12.96 %	25843	14.61 %	24751	10.84 %	24857	11.22 %
rd100	7910	9035	12.45 %	8708	9.16 %	9088	12.96 %	9062	12.71 %
eil101	629	740	15.00 %	731	13.95 %	720	12.64 %	726	13.36 %
lin105	14379	17466	17.67 %	17149	16.15 %	16968	15.26 %	16616	13.46 %
pr124	59030	63859	7.56 %	64806	8.91 %	64998	9.18 %	67139	12.08 %
bier127	118282	140462	15.79 %	141116	16.18 %	142547	17.02 %	139922	15.47 %
ch130	6110	6993	12.63 %	6936	11.91 %	6960	12.21 %	6857	10.89 %
pr136	96772	115122	15.94 %	112504	13.98 %	113532	14.76 %	110596	12.50 %
pr144	58537	63789	8.23 %	65724	10.94 %	66029	11.35 %	66012	11.32 %
kroA150	26524	33285	20.31 %	33897	21.75 %	33870	21.69 %	34631	23.41 %
kroB150	26130	32483	19.56 %	33308	21.55 %	32578	19.79 %	33184	21.26 %
pr152	73682	84881	13.19 %	84819	13.13 %	85237	13.56 %	86964	15.27 %
u159	42080	50776	17.13 %	54142	22.28 %	52220	19.42 %	51686	18.59 %
rat195	2323	3568	34.89 %	3258	28.70 %	3341	30.47 %	3533	34.25 %
kroA200	29368	37345	21.36 %	38861	24.43 %	38629	23.97 %	37628	21.95 %
ts225	126643	167811	24.53 %	159519	20.61 %	155767	18.70 %	156938	19.30 %
tsp225	3919	5389	27.28 %	5392	27.32 %	5134	23.67 %	5184	24.40 %
pr226	80369	91949	12.59 %	92146	12.78 %	92011	12.65 %	88476	9.16 %
Avg. Gap	0.00 %	15.45%		15.30%		15.25%		15.25%	

Table F.5: TSPLib results. The models are trained on TSP20. Augmentation decoding (100) is used.

Instance	Opt. (BKS)	AM		POMO		SymNCO		AM-XL	
		Cost	Gap ↓	Cost	Gap ↓	Cost	Gap ↓	Cost	Gap ↓
eil51	426	445	4.27 %	443	3.84 %	438	2.74 %	441	3.40 %
berlin52	7542	7874	4.22 %	8253	8.62 %	7805	3.37 %	7914	4.70 %
st70	675	696	3.02 %	701	3.71 %	704	4.12 %	696	3.02 %
eil76	538	582	7.56 %	598	10.03 %	574	6.27 %	571	5.78 %
pr76	108159	110726	2.32 %	111534	3.03 %	111035	2.59 %	111416	2.92 %
rat99	1211	1426	15.08 %	1526	20.64 %	1533	21.00 %	1493	18.89 %
kroA100	21282	24327	12.52 %	26154	18.63 %	23784	10.52 %	24798	14.18 %
kroB100	22141	25582	13.45 %	26913	17.73 %	25068	11.68 %	24378	9.18 %
kroC100	20749	23991	13.51 %	22781	8.92 %	23780	12.75 %	23712	12.50 %
kroD100	21294	24289	12.33 %	25099	15.16 %	23815	10.59 %	24052	11.47 %
kroE100	22068	24889	11.33 %	25946	14.95 %	24373	9.46 %	24728	10.76 %
rd100	7910	8738	9.48 %	8840	10.52 %	8674	8.81 %	8419	6.05 %
eil101	629	701	10.27 %	711	11.53 %	706	10.91 %	696	9.63 %
lin105	14379	16670	13.74 %	16956	15.20 %	16297	11.77 %	16656	13.67 %
pr124	59030	63859	7.56 %	66313	10.98 %	62469	5.51 %	62260	5.19 %
bier127	118282	134016	11.74 %	149337	20.80 %	135108	12.45 %	136150	13.12 %
ch130	6110	6816	10.36 %	6995	12.65 %	6732	9.24 %	6791	10.03 %
pr136	96772	113441	14.69 %	112384	13.89 %	110893	12.73 %	109425	11.56 %
pr144	58537	63032	7.13 %	63877	8.36 %	62506	6.35 %	63297	7.52 %
kroA150	26524	32533	18.47 %	33432	20.66 %	32734	18.97 %	31569	15.98 %
kroB150	26130	31116	16.02 %	32583	19.80 %	31105	15.99 %	31246	16.37 %
pr152	73682	81811	9.94 %	81998	10.14 %	81797	9.92 %	81166	9.22 %
u159	42080	51050	17.57 %	52328	19.58 %	50831	17.22 %	50282	16.31 %
rat195	2323	3231	28.10 %	3273	29.03 %	3238	28.26 %	3250	28.52 %
kroA200	29368	36065	18.57 %	38996	24.69 %	36201	18.88 %	37249	21.16 %
ts225	126643	160088	20.89 %	161870	21.76 %	152170	16.78 %	153857	17.69 %
tsp225	3919	5273	25.68 %	5247	25.31 %	5169	24.18 %	5150	23.90 %
pr226	80369	87684	8.34 %	90981	11.66 %	87330	7.97 %	85462	5.96 %
Avg. Gap	0.00 %	12.43%		14.71%		11.82%		11.74%	

Table F.6: TSPLib results. The models are trained on TSP50. Greedy decoding is used.

Instance	Opt. (BKS)	AM		POMO		SymNCO		AM-XL	
		Cost	Gap ↓	Cost	Gap ↓	Cost	Gap ↓	Cost	Gap ↓
eil51	426	440	3.18 %	436	2.29 %	434	1.84 %	436	2.29 %
berlin52	7542	8273	8.84 %	7891	4.42 %	7984	5.54 %	7916	4.72 %
st70	675	694	2.74 %	700	3.57 %	696	3.02 %	686	1.60 %
eil76	538	580	7.24 %	562	4.27 %	572	5.94 %	553	2.71 %
pr76	108159	110798	2.38 %	113731	4.90 %	111953	3.39 %	111360	2.87 %
rat99	1211	1482	18.29 %	1503	19.43 %	1442	16.02 %	1456	16.83 %
kroA100	21282	24457	12.98 %	24102	11.70 %	24345	12.58 %	24115	11.75 %
kroB100	22141	26447	16.28 %	24086	8.08 %	25146	11.95 %	24607	10.02 %
kroC100	20749	24211	14.30 %	23334	11.08 %	22725	8.70 %	23362	11.18 %
kroD100	21294	23117	7.89 %	24180	11.94 %	23326	8.71 %	23751	10.34 %
kroE100	22068	24476	9.84 %	28393	22.28 %	23933	7.79 %	24865	11.25 %
rd100	7910	8163	3.10 %	8139	2.81 %	8072	2.01 %	8082	2.13 %
eil101	629	678	7.23 %	681	7.64 %	691	8.97 %	679	7.36 %
lin105	14379	15590	7.77 %	16418	12.42 %	16545	13.09 %	16029	10.29 %
pr124	59030	61155	3.47 %	61062	3.33 %	59809	1.30 %	59332	0.51 %
bier127	118282	130236	9.18 %	154102	23.24 %	137533	14.00 %	133332	11.29 %
ch130	6110	6440	5.12 %	6441	5.14 %	6308	3.14 %	6320	3.32 %
pr136	96772	104110	7.05 %	104135	7.07 %	103969	6.92 %	102428	5.52 %
pr144	58537	63959	8.48 %	63372	7.63 %	60421	3.12 %	61613	4.99 %
kroA150	26524	30287	12.42 %	30933	14.25 %	30614	13.36 %	30685	13.56 %
kroB150	26130	30565	14.51 %	30997	15.70 %	29083	10.15 %	29528	11.51 %
pr152	73682	84632	12.94 %	79409	7.21 %	78854	6.56 %	78362	5.97 %
u159	42080	46792	10.07 %	46249	9.01 %	46818	10.12 %	44975	6.44 %
rat195	2323	3182	27.00 %	3357	30.80 %	3149	26.23 %	3403	31.74 %
kroA200	29368	35068	16.25 %	37667	22.03 %	35349	16.92 %	34728	15.43 %
ts225	126643	147273	14.01 %	145364	12.88 %	139645	9.31 %	138527	8.58 %
tsp225	3919	4836	18.96 %	5196	24.58 %	4813	18.57 %	5103	23.20 %
pr226	80369	86665	7.26 %	87200	7.83 %	85375	5.86 %	86397	6.98 %
Avg. Gap	0.00 %	10.31%		11.34%		9.11%		9.09%	

Table F.7: TSPLib results. The models are trained on TSP50. Sampling decoding (100 with temperature $\tau = 0.05$) is used.

Instance	Opt. (BKS)	AM		POMO		SymNCO		AM-XL	
		Cost	Gap ↓	Cost	Gap ↓	Cost	Gap ↓	Cost	Gap ↓
eil51	426	440	3.18 %	436	2.29 %	433	1.62 %	436	2.29 %
berlin52	7542	8258	8.67 %	7891	4.42 %	7984	5.54 %	7916	4.72 %
st70	675	694	2.74 %	699	3.43 %	695	2.88 %	686	1.60 %
eil76	538	572	5.94 %	562	4.27 %	570	5.61 %	553	2.71 %
pr76	108159	110798	2.38 %	113034	4.31 %	111953	3.39 %	111360	2.87 %
rat99	1211	1476	17.95 %	1461	17.11 %	1442	16.02 %	1423	14.90 %
kroA100	21282	23863	10.82 %	23674	10.10 %	24230	12.17 %	24115	11.75 %
kroB100	22141	24852	10.91 %	24086	8.08 %	24816	10.78 %	24472	9.53 %
kroC100	20749	23350	11.14 %	23250	10.76 %	22725	8.70 %	23358	11.17 %
kroD100	21294	23117	7.89 %	24103	11.65 %	23326	8.71 %	23720	10.23 %
kroE100	22068	24464	9.79 %	24321	9.26 %	23718	6.96 %	24561	10.15 %
rd100	7910	8092	2.25 %	8070	1.98 %	8068	1.96 %	8014	1.30 %
eil101	629	677	7.09 %	677	7.09 %	684	8.04 %	679	7.36 %
lin105	14379	15559	7.58 %	16369	12.16 %	16073	10.54 %	15520	7.35 %
pr124	59030	61017	3.26 %	60711	2.77 %	59809	1.30 %	59332	0.51 %
bier127	118282	127519	7.24 %	145576	18.75 %	136891	13.59 %	127554	7.27 %
ch130	6110	6354	3.84 %	6399	4.52 %	6291	2.88 %	6308	3.14 %
pr136	96772	103066	6.11 %	103024	6.07 %	103054	6.10 %	101760	4.90 %
pr144	58537	60827	3.76 %	61126	4.24 %	60040	2.50 %	60694	3.55 %
kroA150	26524	30015	11.63 %	30664	13.50 %	30510	13.06 %	30355	12.62 %
kroB150	26130	29521	11.49 %	29313	10.86 %	28883	9.53 %	29029	9.99 %
pr152	73682	80769	8.77 %	78405	6.02 %	77298	4.68 %	77052	4.37 %
u159	42080	45508	7.53 %	45598	7.72 %	46084	8.69 %	44547	5.54 %
rat195	2323	3051	23.86 %	3120	25.54 %	3060	24.08 %	3098	25.02 %
kroA200	29368	34515	14.91 %	35815	18.00 %	33866	13.28 %	34432	14.71 %
ts225	126643	141706	10.63 %	142392	11.06 %	139255	9.06 %	138130	8.32 %
tsp225	3919	4726	17.08 %	4935	20.59 %	4560	14.06 %	4644	15.61 %
pr226	80369	85410	5.90 %	85033	5.48 %	85232	5.71 %	85741	6.27 %
Avg. Gap	0.00 %	8.73%		9.36%		8.27%		7.85%	

Table F.8: TSPLib results. The models are trained on TSP50. Greedy multi-start decoding is used.

Instance	Opt. (BKS)	AM		POMO		SymNCO		AM-XL	
		Cost	Gap ↓	Cost	Gap ↓	Cost	Gap ↓	Cost	Gap ↓
eil51	426	440	3.18 %	431	1.16 %	430	0.93 %	436	2.29 %
berlin52	7542	8270	8.80 %	7679	1.78 %	7984	5.54 %	7731	2.44 %
st70	675	693	2.60 %	693	2.60 %	696	3.02 %	686	1.60 %
eil76	538	580	7.24 %	559	3.76 %	563	4.44 %	553	2.71 %
pr76	108159	110601	2.21 %	111732	3.20 %	111953	3.39 %	111360	2.87 %
rat99	1211	1475	17.90 %	1422	14.84 %	1442	16.02 %	1417	14.54 %
kroA100	21282	23993	11.30 %	23241	8.43 %	23817	10.64 %	24102	11.70 %
kroB100	22141	25097	11.78 %	24071	8.02 %	24026	7.85 %	24607	10.02 %
kroC100	20749	23354	11.15 %	22539	7.94 %	22725	8.70 %	22943	9.56 %
kroD100	21294	23117	7.89 %	23025	7.52 %	22731	6.32 %	23136	7.96 %
kroE100	22068	24476	9.84 %	23746	7.07 %	23908	7.70 %	23834	7.41 %
rd100	7910	8159	3.05 %	8047	1.70 %	8072	2.01 %	8021	1.38 %
eil101	629	666	5.56 %	661	4.84 %	671	6.26 %	661	4.84 %
lin105	14379	15509	7.29 %	15619	7.94 %	16404	12.34 %	15570	7.65 %
pr124	59030	61134	3.44 %	59365	0.56 %	59809	1.30 %	59332	0.51 %
bier127	118282	129821	8.89 %	129934	8.97 %	137100	13.73 %	128116	7.68 %
ch130	6110	6368	4.05 %	6315	3.25 %	6308	3.14 %	6314	3.23 %
pr136	96772	102727	5.80 %	100055	3.28 %	102949	6.00 %	100513	3.72 %
pr144	58537	61943	5.50 %	60386	3.06 %	60421	3.12 %	61131	4.24 %
kroA150	26524	30112	11.92 %	29083	8.80 %	30478	12.97 %	30438	12.86 %
kroB150	26130	29673	11.94 %	29123	10.28 %	28947	9.73 %	28912	9.62 %
pr152	73682	81953	10.09 %	76996	4.30 %	78300	5.90 %	78214	5.79 %
u159	42080	46594	9.69 %	44452	5.34 %	46503	9.51 %	44917	6.32 %
rat195	2323	3095	24.94 %	3075	24.46 %	3088	24.77 %	3100	25.06 %
kroA200	29368	34825	15.67 %	34971	16.02 %	34050	13.75 %	34422	14.68 %
ts225	126643	144315	12.25 %	137942	8.19 %	139548	9.25 %	138438	8.52 %
tsp225	3919	4749	17.48 %	4580	14.43 %	4709	16.78 %	4908	20.15 %
pr226	80369	86582	7.18 %	83980	4.30 %	85375	5.86 %	86237	6.80 %
Avg. Gap	0.00 %	9.24%		7.00%		8.25%		7.72%	

Table F.9: TSPLib results. The models are trained on TSP50. Augmentation decoding (100) is used.

Instance	Opt. (BKS)	AM		POMO		SymNCO		AM-XL	
		Cost	Gap ↓	Cost	Gap ↓	Cost	Gap ↓	Cost	Gap ↓
eil51	426	431	1.16 %	432	1.39 %	429	0.70 %	429	0.70 %
berlin52	7542	7897	4.50 %	7722	2.33 %	7576	0.45 %	7674	1.72 %
st70	675	678	0.44 %	680	0.74 %	678	0.44 %	678	0.44 %
eil76	538	557	3.41 %	559	3.76 %	552	2.54 %	551	2.36 %
pr76	108159	110215	1.87 %	109523	1.25 %	109920	1.60 %	109775	1.47 %
rat99	1211	1435	15.61 %	1436	15.67 %	1412	14.24 %	1424	14.96 %
kroA100	21282	23253	8.48 %	23125	7.97 %	23056	7.69 %	22915	7.13 %
kroB100	22141	23987	7.70 %	23840	7.13 %	23583	6.11 %	23381	5.30 %
kroC100	20749	22041	5.86 %	22458	7.61 %	22504	7.80 %	21706	4.41 %
kroD100	21294	22826	6.71 %	22540	5.53 %	22865	6.87 %	22880	6.93 %
kroE100	22068	23436	5.84 %	23623	6.58 %	23396	5.68 %	23257	5.11 %
rd100	7910	7935	0.32 %	8006	1.20 %	7945	0.44 %	7972	0.78 %
eil101	629	662	4.98 %	665	5.41 %	655	3.97 %	661	4.84 %
lin105	14379	15386	6.54 %	15638	8.05 %	15270	5.83 %	15228	5.58 %
pr124	59030	60586	2.57 %	60150	1.86 %	59565	0.90 %	59332	0.51 %
bier127	118282	124017	4.62 %	129382	8.58 %	127516	7.24 %	125509	5.76 %
ch130	6110	6248	2.21 %	6351	3.79 %	6217	1.72 %	6239	2.07 %
pr136	96772	100325	3.54 %	99948	3.18 %	99458	2.70 %	98595	1.85 %
pr144	58537	60478	3.21 %	59754	2.04 %	59202	1.12 %	59255	1.21 %
kroA150	26524	29298	9.47 %	29127	8.94 %	29587	10.35 %	29278	9.41 %
kroB150	26130	29116	10.26 %	28840	9.40 %	28469	8.22 %	28498	8.31 %
pr152	73682	76378	3.53 %	76074	3.14 %	75825	2.83 %	75495	2.40 %
u159	42080	44124	4.63 %	43795	3.92 %	43765	3.85 %	43846	4.03 %
rat195	2323	3040	23.59 %	3060	24.08 %	3043	23.66 %	2976	21.94 %
kroA200	29368	33751	12.99 %	33743	12.97 %	32690	10.16 %	33660	12.75 %
ts225	126643	140185	9.66 %	139927	9.49 %	139024	8.91 %	138401	8.50 %
tsp225	3919	4633	15.41 %	4624	15.25 %	4528	13.45 %	4622	15.21 %
pr226	80369	83220	3.43 %	83512	3.76 %	83164	3.36 %	83479	3.73 %
Avg. Gap	0.00 %	6.52%		6.61%		5.82%		5.69%	

Table F.10: CVRPLib results. The models are trained on CVRP20. Greedy decoding is used.

Instance	Opt. (BKS)	AM		POMO		SymNCO		AM-XL	
		Cost	Gap ↓	Cost	Gap ↓	Cost	Gap ↓	Cost	Gap ↓
A-n53-k7	1010	1180	14.41 %	1138	11.25 %	1138	11.25 %	1115	9.42 %
A-n54-k7	1167	1272	8.25 %	1351	13.62 %	1300	10.23 %	1303	10.44 %
A-n55-k9	1073	1283	16.37 %	1252	14.30 %	1196	10.28 %	1226	12.48 %
A-n60-k9	1354	1430	5.31 %	1511	10.39 %	1522	11.04 %	1583	14.47 %
A-n61-k9	1034	1186	12.82 %	1222	15.38 %	1201	13.91 %	1244	16.88 %
A-n62-k8	1288	1464	12.02 %	1422	9.42 %	1393	7.54 %	1386	7.07 %
A-n63-k9	1616	1697	4.77 %	1824	11.40 %	1864	13.30 %	1815	10.96 %
A-n63-k10	1314	1371	4.16 %	1577	16.68 %	1536	14.45 %	1549	15.17 %
A-n64-k9	1401	1545	9.32 %	1642	14.68 %	1559	10.13 %	1490	5.97 %
A-n65-k9	1174	1358	13.55 %	1287	8.78 %	1408	16.62 %	1322	11.20 %
A-n69-k9	1159	1345	13.83 %	1360	14.78 %	1319	12.13 %	1334	13.12 %
A-n80-k10	1763	2017	12.59 %	2114	16.60 %	2051	14.04 %	2004	12.03 %
B-n51-k7	1032	1049	1.62 %	1065	3.10 %	1129	8.59 %	1054	2.09 %
B-n52-k7	747	793	5.80 %	893	16.35 %	929	19.59 %	820	8.90 %
B-n56-k7	707	789	10.39 %	815	13.25 %	845	16.33 %	905	21.88 %
B-n57-k7	1153	1375	16.15 %	1401	17.70 %	1435	19.65 %	1340	13.96 %
B-n57-k9	1598	1768	9.62 %	1746	8.48 %	1752	8.79 %	1719	7.04 %
B-n63-k10	1496	1629	8.16 %	1627	8.05 %	1712	12.62 %	1696	11.79 %
B-n64-k9	861	950	9.37 %	997	13.64 %	1065	19.15 %	1098	21.58 %
B-n66-k9	1316	1429	7.91 %	1525	13.70 %	1452	9.37 %	1399	5.93 %
B-n67-k10	1032	1163	11.26 %	1151	10.34 %	1237	16.57 %	1183	12.76 %
B-n68-k9	1272	1463	13.06 %	1498	15.09 %	1444	11.91 %	1476	13.82 %
B-n78-k10	1221	1376	11.26 %	1473	17.11 %	1455	16.08 %	1450	15.79 %
E-n51-k5	521	566	7.95 %	629	17.17 %	621	16.10 %	582	10.48 %
E-n76-k7	682	840	18.81 %	808	15.59 %	847	19.48 %	860	20.70 %
E-n76-k8	735	861	14.63 %	840	12.50 %	884	16.86 %	904	18.69 %
E-n76-k10	830	998	16.83 %	957	13.27 %	986	15.82 %	1047	20.73 %
E-n76-k14	1021	1151	11.29 %	1232	17.13 %	1216	16.04 %	1184	13.77 %
E-n101-k8	815	1113	26.77 %	1051	22.45 %	1183	31.11 %	1101	25.98 %
E-n101-k14	1067	1222	12.68 %	1306	18.30 %	1413	24.49 %	1317	18.98 %
F-n72-k4	237	290	18.28 %	291	18.56 %	404	41.34 %	344	31.10 %
F-n135-k7	1162	1998	41.84 %	2148	45.90 %	2425	52.08 %	2037	42.96 %
M-n101-k10	820	1302	37.02 %	1142	28.20 %	1214	32.45 %	1137	27.88 %
M-n121-k7	1034	1417	27.03 %	1423	27.34 %	2379	56.54 %	1617	36.05 %
M-n151-k12	1015	1284	20.95 %	1374	26.13 %	2013	49.58 %	1582	35.84 %
M-n200-k16	1274	1845	30.95 %	1790	28.83 %	2955	56.89 %	1988	35.92 %
M-n200-k17	1275	1845	30.89 %	1790	28.77 %	2955	56.85 %	1988	35.87 %
Avg. Gap	0.00 %	14.81%		16.60%		21.33%		17.56%	

Table F.11: CVRPLib results. The models are trained on CVRP20. Sampling decoding (100 with temperature $\tau = 0.05$) is used.

Instance	Opt. (BKS)	AM		POMO		SymNCO		AM-XL	
		Cost	Gap ↓	Cost	Gap ↓	Cost	Gap ↓	Cost	Gap ↓
A-n53-k7	1010	1171	13.75 %	1073	5.87 %	1138	11.25 %	1096	7.85 %
A-n54-k7	1167	1257	7.16 %	1257	7.16 %	1299	10.16 %	1271	8.18 %
A-n55-k9	1073	1268	15.38 %	1191	9.91 %	1174	8.60 %	1224	12.34 %
A-n60-k9	1354	1430	5.31 %	1484	8.76 %	1522	11.04 %	1498	9.61 %
A-n61-k9	1034	1112	7.01 %	1183	12.60 %	1136	8.98 %	1202	13.98 %
A-n62-k8	1288	1418	9.17 %	1417	9.10 %	1369	5.92 %	1381	6.73 %
A-n63-k9	1616	1697	4.77 %	1807	10.57 %	1844	12.36 %	1741	7.18 %
A-n63-k10	1314	1366	3.81 %	1443	8.94 %	1441	8.81 %	1488	11.69 %
A-n64-k9	1401	1541	9.09 %	1592	12.00 %	1518	7.71 %	1483	5.53 %
A-n65-k9	1174	1304	9.97 %	1282	8.42 %	1355	13.36 %	1294	9.27 %
A-n69-k9	1159	1303	11.05 %	1288	10.02 %	1272	8.88 %	1317	12.00 %
A-n80-k10	1763	2004	12.03 %	2037	13.45 %	2042	13.66 %	1986	11.23 %
B-n51-k7	1032	1049	1.62 %	1054	2.09 %	1121	7.94 %	1051	1.81 %
B-n52-k7	747	787	5.08 %	805	7.20 %	927	19.42 %	803	6.97 %
B-n56-k7	707	779	9.24 %	789	10.39 %	827	14.51 %	786	10.05 %
B-n57-k7	1153	1366	15.59 %	1253	7.98 %	1238	6.87 %	1326	13.05 %
B-n57-k9	1598	1687	5.28 %	1728	7.52 %	1747	8.53 %	1711	6.60 %
B-n63-k10	1496	1628	8.11 %	1576	5.08 %	1654	9.55 %	1673	10.58 %
B-n64-k9	861	944	8.79 %	974	11.60 %	996	13.55 %	1011	14.84 %
B-n66-k9	1316	1419	7.26 %	1449	9.18 %	1389	5.26 %	1368	3.80 %
B-n67-k10	1032	1161	11.11 %	1095	5.75 %	1132	8.83 %	1169	11.72 %
B-n68-k9	1272	1444	11.91 %	1454	12.52 %	1415	10.11 %	1371	7.22 %
B-n78-k10	1221	1371	10.94 %	1375	11.20 %	1364	10.48 %	1366	10.61 %
E-n51-k5	521	563	7.46 %	562	7.30 %	593	12.14 %	580	10.17 %
E-n76-k7	682	818	16.63 %	795	14.21 %	806	15.38 %	808	15.59 %
E-n76-k8	735	860	14.53 %	824	10.80 %	842	12.71 %	852	13.73 %
E-n76-k10	830	959	13.45 %	939	11.61 %	940	11.70 %	919	9.68 %
E-n76-k14	1021	1148	11.06 %	1147	10.99 %	1141	10.52 %	1139	10.36 %
E-n101-k8	815	1003	18.74 %	1012	19.47 %	1155	29.44 %	1046	22.08 %
E-n101-k14	1067	1214	12.11 %	1302	18.05 %	1286	17.03 %	1297	17.73 %
F-n72-k4	237	290	18.28 %	288	17.71 %	356	33.43 %	311	23.79 %
F-n135-k7	1162	1785	34.90 %	2380	51.18 %	2312	49.74 %	1772	34.42 %
M-n101-k10	820	1127	27.24 %	1159	29.25 %	1137	27.88 %	1104	25.72 %
M-n121-k7	1034	1386	25.40 %	1575	34.35 %	1972	47.57 %	1407	26.51 %
M-n151-k12	1015	1249	18.73 %	1607	36.84 %	2114	51.99 %	1515	33.00 %
M-n200-k16	1274	1652	22.88 %	2424	47.44 %	2802	54.53 %	2013	36.71 %
M-n200-k17	1275	1640	22.26 %	2414	47.18 %	2807	54.58 %	2003	36.35 %
Avg. Gap	0.00 %	12.62%		15.23%		17.96%		14.29%	

Table F.12: CVRPLib results. The models are trained on CVRP20. Greedy multi-start decoding is used.

Instance	Opt. (BKS)	AM		POMO		SymNCO		AM-XL	
		Cost	Gap ↓	Cost	Gap ↓	Cost	Gap ↓	Cost	Gap ↓
A-n53-k7	1010	1078	6.31 %	1038	2.70 %	1059	4.63 %	1069	5.52 %
A-n54-k7	1167	1262	7.53 %	1273	8.33 %	1258	7.23 %	1250	6.64 %
A-n55-k9	1073	1139	5.79 %	1202	10.73 %	1154	7.02 %	1218	11.90 %
A-n60-k9	1354	1430	5.31 %	1442	6.10 %	1482	8.64 %	1508	10.21 %
A-n61-k9	1034	1125	8.09 %	1170	11.62 %	1129	8.41 %	1169	11.55 %
A-n62-k8	1288	1389	7.27 %	1380	6.67 %	1385	7.00 %	1375	6.33 %
A-n63-k9	1616	1689	4.32 %	1762	8.29 %	1789	9.67 %	1760	8.18 %
A-n63-k10	1314	1371	4.16 %	1480	11.22 %	1396	5.87 %	1422	7.59 %
A-n64-k9	1401	1545	9.32 %	1512	7.34 %	1510	7.22 %	1486	5.72 %
A-n65-k9	1174	1243	5.55 %	1286	8.71 %	1344	12.65 %	1285	8.64 %
A-n69-k9	1159	1256	7.72 %	1279	9.38 %	1248	7.13 %	1299	10.78 %
A-n80-k10	1763	1981	11.00 %	2032	13.24 %	1980	10.96 %	1931	8.70 %
B-n51-k7	1032	1049	1.62 %	1052	1.90 %	1081	4.53 %	1044	1.15 %
B-n52-k7	747	791	5.56 %	822	9.12 %	857	12.84 %	800	6.62 %
B-n56-k7	707	757	6.61 %	761	7.10 %	805	12.17 %	774	8.66 %
B-n57-k7	1153	1298	11.17 %	1212	4.87 %	1231	6.34 %	1258	8.35 %
B-n57-k9	1598	1753	8.84 %	1689	5.39 %	1711	6.60 %	1665	4.02 %
B-n63-k10	1496	1629	8.16 %	1560	4.10 %	1624	7.88 %	1635	8.50 %
B-n64-k9	861	947	9.08 %	953	9.65 %	993	13.29 %	998	13.73 %
B-n66-k9	1316	1423	7.52 %	1423	7.52 %	1388	5.19 %	1396	5.73 %
B-n67-k10	1032	1152	10.42 %	1120	7.86 %	1130	8.67 %	1145	9.87 %
B-n68-k9	1272	1410	9.79 %	1443	11.85 %	1334	4.65 %	1352	5.92 %
B-n78-k10	1221	1368	10.75 %	1367	10.68 %	1340	8.88 %	1357	10.02 %
E-n51-k5	521	561	7.13 %	579	10.02 %	590	11.69 %	564	7.62 %
E-n76-k7	682	771	11.54 %	777	12.23 %	822	17.03 %	791	13.78 %
E-n76-k8	735	825	10.91 %	796	7.66 %	861	14.63 %	827	11.12 %
E-n76-k10	830	942	11.89 %	928	10.56 %	950	12.63 %	917	9.49 %
E-n76-k14	1021	1099	7.10 %	1150	11.22 %	1135	10.04 %	1134	9.96 %
E-n101-k8	815	979	16.75 %	979	16.75 %	1117	27.04 %	1042	21.79 %
E-n101-k14	1067	1215	12.18 %	1254	14.91 %	1239	13.88 %	1262	15.45 %
F-n72-k4	237	284	16.55 %	291	18.56 %	359	33.98 %	317	25.24 %
F-n135-k7	1162	1820	36.15 %	1883	38.29 %	2158	46.15 %	1676	30.67 %
M-n101-k10	820	1058	22.50 %	1056	22.35 %	1121	26.85 %	1032	20.54 %
M-n121-k7	1034	1355	23.69 %	1302	20.58 %	1936	46.59 %	1415	26.93 %
M-n151-k12	1015	1274	20.33 %	1309	22.46 %	1856	45.31 %	1435	29.27 %
M-n200-k16	1274	1606	20.67 %	1654	22.97 %	2519	49.42 %	1883	32.34 %
M-n200-k17	1275	1606	20.61 %	1654	22.91 %	2519	49.38 %	1883	32.29 %
Avg. Gap	0.00 %	11.08%		11.78%		16.00%		12.72%	

Table F.13: CVRPLib results. The models are trained on CVRP20. Augmentation decoding (100) is used.

Instance	Opt. (BKS)	AM		POMO		SymNCO		AM-XL	
		Cost	Gap ↓	Cost	Gap ↓	Cost	Gap ↓	Cost	Gap ↓
A-n53-k7	1010	1051	3.90 %	1028	1.75 %	1080	6.48 %	1094	7.68 %
A-n54-k7	1167	1204	3.07 %	1255	7.01 %	1224	4.66 %	1256	7.09 %
A-n55-k9	1073	1139	5.79 %	1153	6.94 %	1155	7.10 %	1174	8.60 %
A-n60-k9	1354	1425	4.98 %	1438	5.84 %	1481	8.58 %	1459	7.20 %
A-n61-k9	1034	1119	7.60 %	1144	9.62 %	1127	8.25 %	1149	10.01 %
A-n62-k8	1288	1349	4.52 %	1410	8.65 %	1374	6.26 %	1376	6.40 %
A-n63-k9	1616	1692	4.49 %	1715	5.77 %	1767	8.55 %	1741	7.18 %
A-n63-k10	1314	1364	3.67 %	1380	4.78 %	1368	3.95 %	1395	5.81 %
A-n64-k9	1401	1490	5.97 %	1501	6.66 %	1513	7.40 %	1490	5.97 %
A-n65-k9	1174	1251	6.16 %	1258	6.68 %	1255	6.45 %	1263	7.05 %
A-n69-k9	1159	1250	7.28 %	1263	8.23 %	1238	6.38 %	1254	7.58 %
A-n80-k10	1763	1907	7.55 %	1937	8.98 %	1946	9.40 %	1928	8.56 %
B-n51-k7	1032	1040	0.77 %	1040	0.77 %	1053	1.99 %	1041	0.86 %
B-n52-k7	747	770	2.99 %	775	3.61 %	755	1.06 %	765	2.35 %
B-n56-k7	707	765	7.58 %	761	7.10 %	769	8.06 %	766	7.70 %
B-n57-k7	1153	1215	5.10 %	1183	2.54 %	1231	6.34 %	1183	2.54 %
B-n57-k9	1598	1655	3.44 %	1656	3.50 %	1681	4.94 %	1635	2.26 %
B-n63-k10	1496	1603	6.67 %	1553	3.67 %	1604	6.73 %	1603	6.67 %
B-n64-k9	861	940	8.40 %	932	7.62 %	922	6.62 %	950	9.37 %
B-n66-k9	1316	1407	6.47 %	1406	6.40 %	1375	4.29 %	1357	3.02 %
B-n67-k10	1032	1113	7.28 %	1095	5.75 %	1096	5.84 %	1097	5.93 %
B-n68-k9	1272	1339	5.00 %	1345	5.43 %	1337	4.86 %	1371	7.22 %
B-n78-k10	1221	1349	9.49 %	1348	9.42 %	1315	7.15 %	1335	8.54 %
E-n51-k5	521	536	2.80 %	565	7.79 %	573	9.08 %	563	7.46 %
E-n76-k7	682	771	11.54 %	747	8.70 %	781	12.68 %	762	10.50 %
E-n76-k8	735	819	10.26 %	805	8.70 %	826	11.02 %	815	9.82 %
E-n76-k10	830	911	8.89 %	919	9.68 %	915	9.29 %	919	9.68 %
E-n76-k14	1021	1097	6.93 %	1109	7.94 %	1131	9.73 %	1114	8.35 %
E-n101-k8	815	948	14.03 %	922	11.61 %	1093	25.43 %	946	13.85 %
E-n101-k14	1067	1184	9.88 %	1212	11.96 %	1219	12.47 %	1225	12.90 %
F-n72-k4	237	274	13.50 %	288	17.71 %	305	22.30 %	291	18.56 %
F-n135-k7	1162	1596	27.19 %	1505	22.79 %	1735	33.03 %	1597	27.24 %
M-n101-k10	820	1017	19.37 %	1015	19.21 %	1089	24.70 %	1061	22.71 %
M-n121-k7	1034	1233	16.14 %	1251	17.35 %	1662	37.79 %	1312	21.19 %
M-n151-k12	1015	1208	15.98 %	1236	17.88 %	1655	38.67 %	1334	23.91 %
M-n200-k16	1274	1559	18.28 %	1668	23.62 %	2360	46.02 %	1815	29.81 %
M-n200-k17	1275	1572	18.89 %	1704	25.18 %	2423	47.38 %	1791	28.81 %
Avg. Gap	0.00 %	8.70%		9.37%		13.00%		10.55%	

Table F.14: CVRPLib results. The models are trained on CVRP50. Greedy decoding is used.

Instance	Opt. (BKS)	AM		POMO		SymNCO		AM-XL	
		Cost	Gap ↓	Cost	Gap ↓	Cost	Gap ↓	Cost	Gap ↓
A-n53-k7	1010	1077	6.22 %	1071	5.70 %	1086	7.00 %	1079	6.39 %
A-n54-k7	1167	1251	6.71 %	1228	4.97 %	1211	3.63 %	1213	3.79 %
A-n55-k9	1073	1166	7.98 %	1107	3.07 %	1158	7.34 %	1203	10.81 %
A-n60-k9	1354	1460	7.26 %	1419	4.58 %	1452	6.75 %	1417	4.45 %
A-n61-k9	1034	1079	4.17 %	1089	5.05 %	1050	1.52 %	1126	8.17 %
A-n62-k8	1288	1367	5.78 %	1385	7.00 %	1369	5.92 %	1331	3.23 %
A-n63-k9	1616	1682	3.92 %	1679	3.75 %	1671	3.29 %	1659	2.59 %
A-n63-k10	1314	1347	2.45 %	1426	7.85 %	1398	6.01 %	1402	6.28 %
A-n64-k9	1401	1493	6.16 %	1436	2.44 %	1469	4.63 %	1469	4.63 %
A-n65-k9	1174	1247	5.85 %	1247	5.85 %	1216	3.45 %	1255	6.45 %
A-n69-k9	1159	1264	8.31 %	1210	4.21 %	1232	5.93 %	1224	5.31 %
A-n80-k10	1763	1864	5.42 %	1923	8.32 %	1921	8.22 %	1881	6.27 %
B-n51-k7	1032	1134	8.99 %	1153	10.49 %	1166	11.49 %	1116	7.53 %
B-n52-k7	747	770	2.99 %	770	2.99 %	809	7.66 %	784	4.72 %
B-n56-k7	707	751	5.86 %	748	5.48 %	813	13.04 %	779	9.24 %
B-n57-k7	1153	1182	2.45 %	1227	6.03 %	1189	3.03 %	1970	41.47 %
B-n57-k9	1598	1670	4.31 %	1686	5.22 %	1660	3.73 %	1660	3.73 %
B-n63-k10	1496	1634	8.45 %	1644	9.00 %	1621	7.71 %	1598	6.38 %
B-n64-k9	861	964	10.68 %	970	11.24 %	972	11.42 %	922	6.62 %
B-n66-k9	1316	1374	4.22 %	1363	3.45 %	1362	3.38 %	1388	5.19 %
B-n67-k10	1032	1137	9.23 %	1148	10.10 %	1135	9.07 %	1189	13.20 %
B-n68-k9	1272	1397	8.95 %	1329	4.29 %	1317	3.42 %	1374	7.42 %
B-n78-k10	1221	1325	7.85 %	1316	7.22 %	1320	7.50 %	1294	5.64 %
E-n51-k5	521	554	5.96 %	582	10.48 %	567	8.11 %	569	8.44 %
E-n76-k7	682	712	4.21 %	744	8.33 %	750	9.07 %	740	7.84 %
E-n76-k8	735	760	3.29 %	816	9.93 %	795	7.55 %	776	5.28 %
E-n76-k10	830	867	4.27 %	901	7.88 %	893	7.05 %	880	5.68 %
E-n76-k14	1021	1075	5.02 %	1076	5.11 %	1133	9.89 %	1115	8.43 %
E-n101-k8	815	920	11.41 %	900	9.44 %	896	9.04 %	892	8.63 %
E-n101-k14	1067	1171	8.88 %	1171	8.88 %	1193	10.56 %	1139	6.32 %
F-n72-k4	237	305	22.30 %	295	19.66 %	320	25.94 %	293	19.11 %
F-n135-k7	1162	1499	22.48 %	1553	25.18 %	1734	32.99 %	2300	49.48 %
M-n101-k10	820	929	11.73 %	917	10.58 %	982	16.50 %	888	7.66 %
M-n121-k7	1034	1209	14.47 %	1300	20.46 %	1373	24.69 %	1177	12.15 %
M-n151-k12	1015	1163	12.73 %	1161	12.58 %	1261	19.51 %	1157	12.27 %
M-n200-k16	1274	1597	20.23 %	1505	15.35 %	1742	26.87 %	1479	13.86 %
M-n200-k17	1275	1597	20.16 %	1505	15.28 %	1742	26.81 %	1479	13.79 %
Avg. Gap	0.00 %	8.42%		8.58%		10.26%		9.69%	

Table F.15: CVRPLib results. The models are trained on CVRP50. Sampling decoding (100 with temperature $\tau = 0.05$) is used.

Instance	Opt. (BKS)	AM		POMO		SymNCO		AM-XL	
		Cost	Gap ↓	Cost	Gap ↓	Cost	Gap ↓	Cost	Gap ↓
A-n53-k7	1010	1072	5.78 %	1071	5.70 %	1086	7.00 %	1079	6.39 %
A-n54-k7	1167	1251	6.71 %	1204	3.07 %	1211	3.63 %	1213	3.79 %
A-n55-k9	1073	1166	7.98 %	1107	3.07 %	1158	7.34 %	1203	10.81 %
A-n60-k9	1354	1457	7.07 %	1408	3.84 %	1448	6.49 %	1417	4.45 %
A-n61-k9	1034	1076	3.90 %	1089	5.05 %	1050	1.52 %	1123	7.93 %
A-n62-k8	1288	1361	5.36 %	1382	6.80 %	1368	5.85 %	1328	3.01 %
A-n63-k9	1616	1670	3.23 %	1679	3.75 %	1667	3.06 %	1659	2.59 %
A-n63-k10	1314	1346	2.38 %	1366	3.81 %	1398	6.01 %	1402	6.28 %
A-n64-k9	1401	1493	6.16 %	1430	2.03 %	1460	4.04 %	1465	4.37 %
A-n65-k9	1174	1241	5.40 %	1229	4.48 %	1216	3.45 %	1255	6.45 %
A-n69-k9	1159	1234	6.08 %	1199	3.34 %	1230	5.77 %	1219	4.92 %
A-n80-k10	1763	1862	5.32 %	1882	6.32 %	1904	7.41 %	1881	6.27 %
B-n51-k7	1032	1134	8.99 %	1153	10.49 %	1166	11.49 %	1116	7.53 %
B-n52-k7	747	769	2.86 %	768	2.73 %	809	7.66 %	784	4.72 %
B-n56-k7	707	751	5.86 %	747	5.35 %	811	12.82 %	762	7.22 %
B-n57-k7	1153	1181	2.37 %	1225	5.88 %	1182	2.45 %	1703	32.30 %
B-n57-k9	1598	1669	4.25 %	1680	4.88 %	1660	3.73 %	1654	3.39 %
B-n63-k10	1496	1634	8.45 %	1592	6.03 %	1620	7.65 %	1598	6.38 %
B-n64-k9	861	955	9.84 %	967	10.96 %	972	11.42 %	922	6.62 %
B-n66-k9	1316	1371	4.01 %	1356	2.95 %	1362	3.38 %	1383	4.84 %
B-n67-k10	1032	1136	9.15 %	1142	9.63 %	1133	8.91 %	1180	12.54 %
B-n68-k9	1272	1383	8.03 %	1324	3.93 %	1317	3.42 %	1374	7.42 %
B-n78-k10	1221	1325	7.85 %	1285	4.98 %	1316	7.22 %	1294	5.64 %
E-n51-k5	521	551	5.44 %	574	9.23 %	565	7.79 %	569	8.44 %
E-n76-k7	682	707	3.54 %	738	7.59 %	744	8.33 %	740	7.84 %
E-n76-k8	735	760	3.29 %	816	9.93 %	786	6.49 %	774	5.04 %
E-n76-k10	830	862	3.71 %	895	7.26 %	893	7.05 %	876	5.25 %
E-n76-k14	1021	1075	5.02 %	1076	5.11 %	1128	9.49 %	1105	7.60 %
E-n101-k8	815	894	8.84 %	891	8.53 %	890	8.43 %	888	8.22 %
E-n101-k14	1067	1171	8.88 %	1161	8.10 %	1166	8.49 %	1138	6.24 %
F-n72-k4	237	305	22.30 %	293	19.11 %	307	22.80 %	289	17.99 %
F-n135-k7	1162	1453	20.03 %	1521	23.60 %	1557	25.37 %	2141	45.73 %
M-n101-k10	820	927	11.54 %	915	10.38 %	969	15.38 %	888	7.66 %
M-n121-k7	1034	1145	9.69 %	1276	18.97 %	1347	23.24 %	1121	7.76 %
M-n151-k12	1015	1148	11.59 %	1128	10.02 %	1228	17.35 %	1120	9.38 %
M-n200-k16	1274	1520	16.18 %	1486	14.27 %	1642	22.41 %	1462	12.86 %
M-n200-k17	1275	1558	18.16 %	1475	13.56 %	1664	23.38 %	1460	12.67 %
Avg. Gap	0.00 %	7.71%		7.70%		9.40%		8.88%	

Table F.16: CVRPLib results. The models are trained on CVRP50. Greedy multi-start decoding is used.

Instance	Opt. (BKS)	AM		POMO		SymNCO		AM-XL	
		Cost	Gap ↓	Cost	Gap ↓	Cost	Gap ↓	Cost	Gap ↓
A-n53-k7	1010	1063	4.99 %	1061	4.81 %	1071	5.70 %	1059	4.63 %
A-n54-k7	1167	1217	4.11 %	1188	1.77 %	1201	2.83 %	1211	3.63 %
A-n55-k9	1073	1116	3.85 %	1096	2.10 %	1117	3.94 %	1144	6.21 %
A-n60-k9	1354	1410	3.97 %	1393	2.80 %	1390	2.59 %	1379	1.81 %
A-n61-k9	1034	1067	3.09 %	1077	3.99 %	1050	1.52 %	1082	4.44 %
A-n62-k8	1288	1346	4.31 %	1348	4.45 %	1354	4.87 %	1331	3.23 %
A-n63-k9	1616	1682	3.92 %	1659	2.59 %	1668	3.12 %	1657	2.47 %
A-n63-k10	1314	1347	2.45 %	1336	1.65 %	1362	3.52 %	1348	2.52 %
A-n64-k9	1401	1486	5.72 %	1426	1.75 %	1438	2.57 %	1461	4.11 %
A-n65-k9	1174	1231	4.63 %	1220	3.77 %	1216	3.45 %	1226	4.24 %
A-n69-k9	1159	1189	2.52 %	1189	2.52 %	1200	3.42 %	1209	4.14 %
A-n80-k10	1763	1845	4.44 %	1834	3.87 %	1840	4.18 %	1811	2.65 %
B-n51-k7	1032	1038	0.58 %	1037	0.48 %	1078	4.27 %	1078	4.27 %
B-n52-k7	747	769	2.86 %	764	2.23 %	797	6.27 %	768	2.73 %
B-n56-k7	707	748	5.48 %	743	4.85 %	786	10.05 %	774	8.66 %
B-n57-k7	1153	1177	2.04 %	1171	1.54 %	1169	1.37 %	1680	31.37 %
B-n57-k9	1598	1662	3.85 %	1651	3.21 %	1655	3.44 %	1642	2.68 %
B-n63-k10	1496	1612	7.20 %	1590	5.91 %	1606	6.85 %	1598	6.38 %
B-n64-k9	861	936	8.01 %	943	8.70 %	939	8.31 %	922	6.62 %
B-n66-k9	1316	1365	3.59 %	1348	2.37 %	1351	2.59 %	1376	4.36 %
B-n67-k10	1032	1123	8.10 %	1111	7.11 %	1128	8.51 %	1137	9.23 %
B-n68-k9	1272	1345	5.43 %	1315	3.27 %	1312	3.05 %	1351	5.85 %
B-n78-k10	1221	1289	5.28 %	1278	4.46 %	1298	5.93 %	1288	5.20 %
E-n51-k5	521	554	5.96 %	533	2.25 %	553	5.79 %	567	8.11 %
E-n76-k7	682	711	4.08 %	719	5.15 %	742	8.09 %	707	3.54 %
E-n76-k8	735	760	3.29 %	770	4.55 %	765	3.92 %	776	5.28 %
E-n76-k10	830	854	2.81 %	870	4.60 %	890	6.74 %	878	5.47 %
E-n76-k14	1021	1062	3.86 %	1059	3.59 %	1078	5.29 %	1073	4.85 %
E-n101-k8	815	893	8.73 %	890	8.43 %	885	7.91 %	890	8.43 %
E-n101-k14	1067	1154	7.54 %	1155	7.62 %	1182	9.73 %	1139	6.32 %
F-n72-k4	237	295	19.66 %	268	11.57 %	294	19.39 %	290	18.28 %
F-n135-k7	1162	1414	17.82 %	1409	17.53 %	1554	25.23 %	1984	41.43 %
M-n101-k10	820	877	6.50 %	892	8.07 %	922	11.06 %	886	7.45 %
M-n121-k7	1034	1151	10.17 %	1234	16.21 %	1352	23.52 %	1113	7.10 %
M-n151-k12	1015	1146	11.43 %	1141	11.04 %	1256	19.19 %	1118	9.21 %
M-n200-k16	1274	1537	17.11 %	1477	13.74 %	1629	21.79 %	1453	12.32 %
M-n200-k17	1275	1537	17.05 %	1477	13.68 %	1629	21.73 %	1453	12.25 %
Avg. Gap	0.00 %	6.39%		5.63%		7.88%		7.61%	

Table F.17: CVRPLib results. The models are trained on CVRP50. Augmentation decoding (100) is used.

Instance	Opt. (BKS)	AM		POMO		SymNCO		AM-XL	
		Cost	Gap ↓	Cost	Gap ↓	Cost	Gap ↓	Cost	Gap ↓
A-n53-k7	1010	1045	3.35 %	1046	3.44 %	1062	4.90 %	1064	5.08 %
A-n54-k7	1167	1200	2.75 %	1181	1.19 %	1197	2.51 %	1176	0.77 %
A-n55-k9	1073	1090	1.56 %	1107	3.07 %	1104	2.81 %	1117	3.94 %
A-n60-k9	1354	1378	1.74 %	1392	2.73 %	1389	2.52 %	1380	1.88 %
A-n61-k9	1034	1058	2.27 %	1050	1.52 %	1050	1.52 %	1065	2.91 %
A-n62-k8	1288	1334	3.45 %	1329	3.09 %	1330	3.16 %	1321	2.50 %
A-n63-k9	1616	1655	2.36 %	1651	2.12 %	1659	2.59 %	1659	2.59 %
A-n63-k10	1314	1339	1.87 %	1358	3.24 %	1344	2.23 %	1351	2.74 %
A-n64-k9	1401	1442	2.84 %	1434	2.30 %	1435	2.37 %	1443	2.91 %
A-n65-k9	1174	1205	2.57 %	1206	2.65 %	1199	2.09 %	1217	3.53 %
A-n69-k9	1159	1201	3.50 %	1199	3.34 %	1186	2.28 %	1196	3.09 %
A-n80-k10	1763	1811	2.65 %	1843	4.34 %	1816	2.92 %	1822	3.24 %
B-n51-k7	1032	1026	-0.58 %	1027	-0.49 %	1031	-0.10 %	1025	-0.68 %
B-n52-k7	747	763	2.10 %	759	1.58 %	763	2.10 %	758	1.45 %
B-n56-k7	707	736	3.94 %	723	2.21 %	741	4.59 %	732	3.42 %
B-n57-k7	1153	1167	1.20 %	1159	0.52 %	1175	1.87 %	1166	1.11 %
B-n57-k9	1598	1651	3.21 %	1634	2.20 %	1625	1.66 %	1623	1.54 %
B-n63-k10	1496	1581	5.38 %	1580	5.32 %	1576	5.08 %	1587	5.73 %
B-n64-k9	861	930	7.42 %	920	6.41 %	920	6.41 %	922	6.62 %
B-n66-k9	1316	1349	2.45 %	1338	1.64 %	1345	2.16 %	1359	3.16 %
B-n67-k10	1032	1073	3.82 %	1061	2.73 %	1069	3.46 %	1088	5.15 %
B-n68-k9	1272	1312	3.05 %	1323	3.85 %	1317	3.42 %	1346	5.50 %
B-n78-k10	1221	1265	3.48 %	1286	5.05 %	1277	4.39 %	1269	3.78 %
E-n51-k5	521	535	2.62 %	547	4.75 %	545	4.40 %	551	5.44 %
E-n76-k7	682	707	3.54 %	718	5.01 %	712	4.21 %	717	4.88 %
E-n76-k8	735	753	2.39 %	761	3.42 %	759	3.16 %	763	3.67 %
E-n76-k10	830	847	2.01 %	863	3.82 %	861	3.60 %	859	3.38 %
E-n76-k14	1021	1052	2.95 %	1049	2.67 %	1068	4.40 %	1073	4.85 %
E-n101-k8	815	866	5.89 %	874	6.75 %	887	8.12 %	869	6.21 %
E-n101-k14	1067	1136	6.07 %	1143	6.65 %	1157	7.78 %	1131	5.66 %
F-n72-k4	237	271	12.55 %	269	11.90 %	266	10.90 %	281	15.66 %
F-n135-k7	1162	1307	11.09 %	1358	14.43 %	1390	16.40 %	1364	14.81 %
M-n101-k10	820	873	6.07 %	905	9.39 %	891	7.97 %	851	3.64 %
M-n121-k7	1034	1129	8.41 %	1225	15.59 %	1149	10.01 %	1116	7.35 %
M-n151-k12	1015	1112	8.72 %	1126	9.86 %	1190	14.71 %	1103	7.98 %
M-n200-k16	1274	1473	13.51 %	1430	10.91 %	1580	19.37 %	1430	10.91 %
M-n200-k17	1275	1482	13.97 %	1466	13.03 %	1580	19.30 %	1416	9.96 %
Avg. Gap	0.00 %	4.49%		4.93%		5.44%		4.77%	